Check for updates

A new strategy for the extrahepatic delivery of lipid-based nanomedicines: a protein corona-mediated selective targeting system based on an ionizable cationic lipid library

Mahmoud A. Younis, [ID] [a,b,c] Yusuke Sato, [a,b,d] Seigo Kimura [ID] [e] and Hideyoshi Harashima [ID] *[a,b]

Applying lipid nanoparticle (LNP) technology to ribonucleic acid (RNA) nanomedicines was integral to the success of mRNA vaccines against COVID-19. To expand the power of LNP technology, extrahepatic delivery systems have been developed using specific ligands that target the cells in question. However, recent increases in evidence support targeting without the need to attach specific ligands to nanocarriers. In this review, we focused on protein corona-mediated extrahepatic delivery of nanoparticles as an alternative to classic ligand-mediated active targeting. First, the interaction of LNPs with biological components and the impact that the physicochemical properties of LNPs exert on their biological fate are discussed. Then, we highlight a new system that targets activated hepatic stellate cells (aHSCs) as a successful model achieved through intensive optimization of LNPs based on an ionizable cationic lipid library. We also discuss cumulative evidence that support the ligand-free extrahepatic delivery of nanoparticles to a broad diversity of tissues, such as the spleen, lungs, brain, tumors, kidneys, placenta, pancreas, and bone marrow. In conclusion, we propose protein corona-mediated extrahepatic delivery as a new strategy of active targeting for RNA nanomedicines and inspire the future directions in this area.

1. Introduction

Lipid nanoparticles (LNPs) have recently revolutionized the field of drug delivery owing to their versatile applicability to the delivery of diverse cargoes that range from small molecules to large nucleic acids and proteins.[1] Furthermore, LNP-based vaccines saved millions of lives during the COVID-19 pandemic.[2] Interest in the impact of the composition of LNPs on their *in vivo* performance has undergone growth recently—particularly in the area of gene delivery. While the main lipids (*e.g.*, cationic or ionizable lipids) have received much attention as the fundamental functional components of LNPs, a substantially lower level of interest has been directed to helper lipids. Helper lipids are secondary components of LNPs, and they include a diverse array of lipids and lipid-like materials, such as phospholipids, cholesterol, or polyethylene glycol (PEG)-modified lipids. These are often incorporated into LNPs to assist with colloidal stability, control pharmacokinetics, or promote the escape of cargoes from lysosomal degradation.[3] Apart from their classic role, recent reports have revealed the significant impact of helper lipids on the *in vivo* biodistribution of LNPs and subsequent intracellular events.[4,5]

Active targeting has been the main strategy to achieve cell-specific delivery of nanomedicines during the past two decades.[6,7] By exploiting the differential expressions of certain receptors or unique features in the microenvironments of target cells (*e.g.* pH, redox potential, enzymatic activity, *etc.*), nanocarriers are equipped with targeting moieties that either bind to these receptors or respond to such specific features to increase their affinity to the cells in question.[8] A wide variety of targeting moieties have been investigated, ranging from small ligands to antibodies and chemical linkers.[9,10] Despite their promising potential *in vitro*, the *in vivo* application of ligand-based delivery systems is challenged by multiple obstacles, including their poor stability in biological fluids, improper pharmacokinetic performance, immunogenicity, and difficulties in controlling ligand–receptor binding in the

[a]*Laboratory of Innovative Nanomedicine, Faculty of Pharmaceutical Sciences, Hokkaido University, Sapporo 060-0812, Japan. E-mail: harasima@pharm.hokudai.ac.jp*

[b]*Institute of Vaccine Research and Development (IVReD), Hokkaido University, Kita 21, Nishi 11, Kita-ku, Sapporo 001-0021, Japan*

[c]*Department of Industrial Pharmacy, Faculty of Pharmacy, Assiut University, Assiut 71526, Egypt*

[d]*Laboratory for Molecular Design of Pharmaceutics, Faculty of Pharmaceutical Sciences, Hokkaido University, Sapporo 060-0812, Japan*

[e]*Integrated Research Consortium on Chemical Science, Graduate School of Science, Nagoya University, Nagoya 464-8602, Japan*

dynamic three-dimensional *in vivo* environment, which is much more complicated than the static two-dimensional cell culture models. Moreover, the scale-up of such delivery systems is limited by their intricacy and multiple preparation steps. Collectively, the abovementioned factors reduce the clinical translatability of ligand-based nanocarriers.[11] Thus, innovative targeting approaches are necessary to cope with the aforementioned challenges.

Recently, the role of the "protein corona" has been recognized as an important factor in the *in vivo* distribution of LNPs[12] since LNPs are covered with plasma/serum proteins once they enter blood circulation. Hajipour M. J. *et al.* reported on 4022 unique proteins that were identified on nanoparticles based on a literature search using physicochemical properties, sizes, and protein sources.[13] There is increasing information available on the relationship between certain components of the protein corona and tissue distribution of nanoparticles, such as that for the liver (apolipoprotein E; ApoE), lung (serum albumin and ApoE), spleen (complements and immunoglobulins such as opsonins), and brain (ApoE4 and ApoB-100).[14] Therefore, a new strategy has emerged for tissue-selective targeting based on the protein corona as an endogenous ligand without the external introduction of artificial ligands.[15]

In this review, we first explore the molecular mechanisms of interactions between nanoparticles and biological components from the viewpoint of using a library of ionizable cationic lipids. Subsequently, we highlight a successful case study in which an active targeting system to the activated hepatic stellate cells (aHSCs), a model of a specific minor cellular population, was developed for potential clinical applicability in the treatment of liver fibrosis. Furthermore, we summarize recent strategies for protein corona-mediated delivery to various extrahepatic tissues, such as the spleen, the lungs, the brain, tumors, kidneys, the placenta, the pancreas, and bone marrow. Finally, we inspire future perspectives in this research area.

2. Understanding the interactions between nanoparticles and biological components

Active targeting is a straightforward approach where ligands as receptors and other proteins expressed on the surface of target cells are decorated on the surface of LNPs. Decorating LNPs with small molecular ligands, peptides or antibodies is not a novel approach.[16] Conversely, ligand-decorated nanoparticle formulations are yet to be approved for practical use. Although it is difficult to identify the specific causes for this lack of acceptance, the complexity of the formulation process and formulation characterization, along with the increased cost of formulation, all are likely factors. Currently, it is impossible to completely eliminate interactions between nanoparticles and biological components.[17,18] Thus, interactions other than the desired ligand–receptor types could occur with ligand-decorated nanoparticles. The lack of adequate control during dynamic and complex interactions involving very large numbers of proteins is likely the main reason for the above problems. Nevertheless, it is becoming clearer that physicochemical properties such as particle size and charge are quite relevant to the *in vivo* fate of LNPs.[16] The following section lists the results of our study, along with recently established evidence of nanoparticle interactions with biological components, and the relationships between physicochemical properties and the *in vivo* fate of LNPs.

Dr Mahmoud A. Younis is a Specially Appointed Assistant Professor at Hokkaido University Institute of Vaccine Research and Development (IVReD), Japan. He completed his PhD and postdoctoral training in nucleic acid drug delivery systems at Hokkaido University under the supervision of Prof. Hideyoshi Harashima. His research focuses on the application of nucleic acid therapeutics in the treatment of various health chal-

Mahmoud A. Younis

lenges, including cancer and liver diseases, as well as the development of mRNA vaccines using lipid nanoparticle technology. Moreover, he works on the development of novel targeting approaches that recruit the endogenous pathways in the body, rather than the classic ligand-based targeting.

Yusuke SATO is an Associate Professor in the Faculty of Pharmaceutical Sciences, Hokkaido University. His main research interest is the development of potent lipid nanoparticles for the in vivo delivery of macromolecules, including short interfering RNAs (siRNAs), mRNAs, and clustered regularly interspaced short palindromic repeats (CRISPR)-associated (Cas) ribonucleoproteins (RNPs), based on the molecular design of

Yusuke Sato

functional lipids, including ionizable lipids and zwitterionic lipids. He promotes industry-academia collaboration activities with the aim of implementing the use of his lipids and formulation technologies in collaboration with the Institute for the Promotion of Business-Regional Collaboration at Hokkaido University and private sector companies.

2.1. Biomolecular corona

Nanoparticles exhibit a so-called "synthetic identity", which is a property that is determined by the chemical structures and combinations of the components, along with the manufacturing process. Once a nanoparticle is administered into a living organism, proteins and other biological components adsorb onto the nanoparticle interface, which forms a biomolecular corona that exhibits a so-called "biological identity" that is defined by its properties. Incorrect control of the biomolecular corona, which is a platform for *in situ* decoration of the synthesized nanoparticles, reduces the quality of active targeting. In contrast, intended control not only increases the quality of active targeting, it programs the expected targeting ability in nanoparticles that are not artificially ligand-decorated.[19] According to the Vroman effect, the nanoparticle interface is initially dominated by proteins that are present in high concentrations in the surroundings, and the proteins with lower affinity to the nanoparticles are replaced over time by proteins in lower concentrations with higher affinity.[20] The composition of a biomolecular corona under static *in vitro* conditions differs when under dynamic *in vivo* conditions due to the effect of shear stress on the nanoparticles.[21,22] The composition of a biomolecular corona differs depending on whether it is located in the plasma, serum or whole blood.[23,24] The type of anti-coagulant agent used to obtain plasma also affects the composition of the biomolecular corona.[25] Furthermore, differences in the plasma proteome due to disease and individual differences also influence the composition of the biomolecular corona.[26,27] Thus, the biological identity of nanoparticles is not necessarily tied to their synthetic identity because the aforementioned complicating factors are involved (Fig. 1). Naturally, the route of administration would also affect the biomolecular corona due to the fact that the pro-

teome is completely different between biological fluids, and because components of the biomolecular corona change after nanoparticles translocate into a different biological fluid.[28] However, because the biomolecular corona is often highly enriched with very low concentrations of proteins, attempts are often made to use the proteome of the biomolecular corona formed in a given nanoparticle as a useful tool for detecting or identifying pathologies with better sensitivity than what could be accomplished using the plasma proteome.[29]

LNPs are predominantly composed of lipids. Although various models have been proposed for an improved internal structure, these generally represent a structure with a large number of lipid molecules inside.[30] Although the specific gravity of LNPs becomes slightly higher when nucleic acids are encapsulated, these forms are much lighter than that of nanoparticles made of harder materials.[31] Therefore, LNPs exhibit specific gravity similar to that of the various lipoproteins and extracellular vesicles present in blood. In addition, the particle sizes of these endogenous vesicles and LNPs are within a similar range. Therefore, it is assumed to be difficult to highly purify corona-formed LNPs from biological fluids by using a single separation method, such as size exclusion chromatography (SEC) or centrifugation. The conventional approach dictates that either a combination or the optimization of these methods is necessary.[32] At least two studies have reported on affinity purification methods using antibodies against polyethylene glycol (PEG); these methods typically use polymers to control the particle size of LNPs and improve their stability in blood.[33,34] In other reports, Francia V. *et al.* demonstrated that magnetic iron-oxide-loaded LNPs (IOLNP) allow for separation of LNP-corona complexes from biological media through magnetic separation,[35] and Baimanov D. *et al.* developed a rapid affinity-based technique achieved by chemically immobilizing

Seigo Kimura

Dr Seigo Kimura is an Assistant Professor at Nagoya University and a Specially Appointed Assistant Professor at Kyoto University. He earned his Ph.D. in Pharmaceutical Sciences from Hokkaido University under Prof. Hideyoshi Harashima. His research focuses on lipid-based nanoparticles (LNPs) for targeted nucleic acid delivery in vivo, enabling gene therapy, cancer immunotherapy, and vaccination. At Nagoya University, he investigates chemically modified and circular RNAs for therapeutic applications. At Kyoto University, he develops peptide-based and peptide–lipid hybrid systems to enhance intracellular delivery. His work bridges material design with in vivo biology to advance next-generation RNA therapeutics and delivery technologies.

Hideyoshi Harashima

Hideyoshi Harashima is a Distinguished Professor at the Laboratory of Innovative Nanomedicine, Faculty of Pharmaceutical Sciences, Hokkaido University. He received his Ph.D. from The University of Tokyo. After his postdoctoral training at Stanford University, he became an Associate Professor at the University of Tokushima in 1989. He was appointed as a Full Professor of Laboratory for Molecular Design of Pharmaceutics at Hokkaido University from 1999 until 2023. Currently, he is appointed Professor of a newly build Laboratory of Innovative Nanomedicine in 2009. He has published 472 original research articles and 72 invited reviews. He received the Høst Madsen Medal from FIP in 2021.
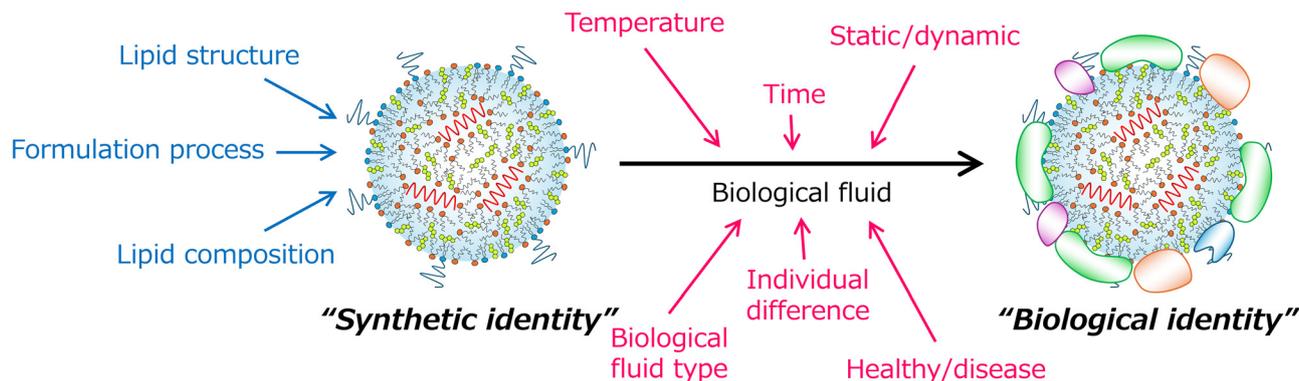
Fig. 1 Various factors on synthetic and biological identity. Owing to the influence of various conditions, including the type of biological fluid and temperature, the biological identity of nanoparticles is not necessarily paired with the synthetic identity.

LNPs *via* carbodiimide cross-linking on the surface of biosensors.[36] The development of such new purification approaches is expected to facilitate future elucidation of the biomolecular corona of LNPs. In addition, a number of studies have reported analyses of the biomolecular corona *via* LNP purification from biological fluid using only simple centrifugation or SEC.[37–39] Criteria assuring the quality of the samples measured are considered to be future issues. From another perspective, it has also been noted that the results of analyses differ depending on the facility under which the proteome analysis is performed, and comparisons between independent reports should understandably proceed with caution.[40]

2.2. Physicochemical properties of LNPs that affect the *in vivo* fate: impact of the lipid library

LNPs are typically composed of ionizable lipids, phospholipids, cholesterol, and PEG-lipids. As mentioned above, the *in vivo* fate of LNPs is controlled by the chemical structure of the lipid components. In this section, the effects of ionizable lipids and phospholipids are described, and the effects of the fundamental physicochemical properties such as charge and particle size also are discussed.

Phospholipids are the structural lipids in LNPs, and are preferentially localized at the interface of LNPs due to their relatively bulky hydrophilic head group.[41] Therefore, their chemical structure and content has a significant impact on the interfacial properties of the LNPs. Chander *et al.* found that when the phospholipids in LNPs were replaced with egg sphingomyelin (ESM), their content could be increased by 40 mol%, which resulted in decreases and increases in functional mRNA delivery in the liver and secondary lymphatic tissues (spleen and bone marrow), respectively, compared with LNPs containing the typical 10 mol% of 1,2-distearoyl-3-*sn-glycero*-phosphocholine (DSPC).[42] The ESM improved both blood stability and blood half-life, which is attributed to increases in the opportunities for mRNA delivery into extrahepatic tissues. Hashiba *et al.* compared DSPC content from 5 to 25 mol% and found that LNPs containing 25 mol% DSPC improved the functional mRNA delivery to extrahepatic tissues, including the spleen,

the lungs, and kidneys.[43] Substitution of DSPC with DSPG biocentrically tilts the selectivity of LNPs towards reticuloendothelial system (RES) cells, which includes liver sinusoidal endothelial cells (LSECs) and Kupffer cells.[44] Since phospholipids are also involved in the pH-change-induced reorganization of LNPs and have significant impact on the level of functional mRNA delivery,[45] the role of phospholipids in enhancing function and diversifying applicability of the LNPs will be significant in the future.

Recently, Fei *et al.* proposed a SELECT platform (simplified LNP with engineered mRNA for cell-type targeting), which is different from the usual LNP without phospholipids, that can still deliver mRNA to the lung effectively.[46] They started from a 5-component system (SM-102, DOTAP, DSPC, Chol, PEG) and found no effect of DSPC on the transfection activity in the lung. They examined a 4-component system (SM-102, DOTAP, Chol, PEG) excluding DSPC, and found no effect of cholesterol. Finally, they found that a 3-component system (SM-102, DOTAP, PEG) can exert the highest transfection activity in the lung compared to those of the 4- and 5-component systems. Therefore, the precise role of phospholipids in the transfection activity of mRNA should be carefully examined in each tissue of concern with specified ionizable lipids.

The apparent value for the acid dissociation constant (pK_a) of LNPs could be controlled depending on the chemical structure of the ionizable lipids.[47,48] The pK_a is an important property for functional RNA delivery, and has an optimal range of 6.2–6.5 in the liver.[49] Sato *et al.* have developed various ionizable lipid libraries with a wide range of pK_a values, and reported the effects on both the cell and tissue selectivity of LNPs. Comparisons of the intrahepatic distribution of LNPs with different pK_a values have shown that LNPs with a pK_a below 6.0 selectively accumulated in liver parenchymal cells, and showed a significant change in selectivity towards liver sinusoidal endothelial cells (LSECs) and even Kupffer cells with increases in the pK_a.[47] Modulation of the pK_a by a combination of two ionizable lipids with different pK_a values results in similar LSEC-specific accumulation and gene silencing after siRNA delivery, suggesting that the LSEC-tropic properties of

the LNPs are pK_a-dependent rather than ionizable lipid chemical structure-dependent.[50] Compared with the aforementioned DSPG-LNPs, the signs of the charges are opposite, which suggests different accumulation mechanisms. By using our original ionizable lipid library, Younis *et al.* showed that activated hepatic stellate cells (aHSC) efficiently take up LNPs with a pK_a of around 7.[5,51] This pK_a range is similar to what is optimal for LSECs, but the use of 1,2-dioleoyl-3-*sn*-glycero-phosphoethanolamine (DOPE) as a phospholipid was also important. Interestingly, the same LNPs were also shown to be spleen-tropic in healthy mice, but aHSC-tropic only in liver-fibrosis models. This phenomenon could be due to changes in the biomolecular corona associated with plasma proteome changes during pathological conditions (*i.e.*, changes in the biological identity of LNPs), as described above. Furthermore, Hashiba *et al.* developed an ionizable-lipid library that focuses on branched scaffold structures, which includes the total carbon number and symmetry. The results found in this library suggest that the symmetry of branching significantly contributes to physical stability during storage and fusogenicity. Interestingly, these results suggest that the structure of ionizable lipids, specifically the total carbon number of branched scaffolds, significantly changes the tissue tropism of functional mRNA delivery between the liver and the spleen.[52] The fact that the head structure of ionizable lipids is constant and that there is no significant difference in the pK_a of LNPs suggests that any change in biological identity could be due to changes in membrane fluidity or to other physicochemical properties.

The particle size of LNPs has a significant impact on functional RNA delivery, and reducing the diameter of LNPs to below ~50 nm significantly reduces the level of functional RNA delivery, which is only observed in the presence of serum.[47,53,54] While this could be explained as membrane destabilization due to sparse lipid packing and increased interfacial energy with decreasing particle size, differences in the biomolecular corona are also suggested. Indeed, the effect of particle size on the biomolecular corona of nanoparticles made of various materials has been clarified.[55,56] In particular, the larger the particle size, the greater the amount of protein adsorbed and the thicker the corona layer.[55] A correlation between the amount of protein and cellular uptake has also been reported. Adsorption of immunoglobulin also results in a complement reaction on the nanoparticle interface, which promotes uptake into phagocytes (*i.e.*, clearance from the blood) *via* the complement pathway.[57,58] We have shown that the particle size of RNA-loaded LNPs could be largely controlled by adjusting either the amount of PEG modification or the salt concentration during the manufacturing process, which leads to increased levels of functional RNA delivery to peritoneal macrophages or to splenic dendritic cells following either intraperitoneal or intravenous administration, respectively.[59–61] Kranz *et al.* have shown that mRNA-lipoplexes with diameters of approximately 200 nm, and without ligand decoration, efficiently delivered mRNA into splenic dendritic cells, and clinical trials are underway by BioNTech as mRNA

cancer vaccines for melanoma patients.[62,63] The particle size of mRNA-LNPs also appears to influence the induction of antigen-specific antibody expression following intramuscular administration.[64]

Thus, the chemical structure and physical properties are positively correlated with the *in vivo* fate of nanoparticles. An understanding of the biomolecular corona reveals these correlations. The chemical space of nanoparticles is practically infinite, and currently only a small fraction of it has been explored. Although this indicates the enormous potential of nanoparticles, it would be difficult to randomly explore all of them. It is important to search for nanoparticle formulations that show efficient and useful properties *via* biocentric approaches and machine learning based on inspiration from researchers.

3. Modifying nanocarriers for ligand-free targeting of specific cellular populations: a successful case study

Tremendous efforts have been exerted toward understanding the mechanisms and composition of nanomedicines-associated protein coronas, as well as the impact of this phenomenon on the *in vivo* fate of nanocarriers, which includes their stability, biodistribution, and biosafety.[65,66] A growing amount of evidence shows that the composition of the protein corona varies depending on the nature of the nanocarrier, which subsequently affects the *in vivo* performance of the nanocarrier in question. Thus, the concept of protein corona-based targeting has come to the forefront.[10,67] By modifying the composition and physico-chemical properties of nanocarriers, the nature of the protein corona can be manipulated to harness the endogenous transport pathways for a ligand-free targeting of the cells in question. Thus, the necessity of attaching targeting ligands to the LNPs could be eliminated to promote the scalability and clinical translatability of the developed nanocarriers.[11] This concept could be applied to target certain tissues (*e.g.*, liver, spleen, or lung), or even to selectively target specific cellular populations within the tissue of interest.

Liver fibrosis is a chronic disorder that can proceed into irreversible and life-threatening complications. Activated hepatic stellate cells (aHSCs) are the fundamental players in the development and progression of liver fibrosis. In response to a chronic liver injury, the hepatic stellate cells transform from a quiescent phenotype (qHSCs) into activated myofibroblasts (aHSCs), with a subsequent deposition of extracellular matrix (ECM).[68,69] While gene therapy sounds promising for the treatment of liver diseases, the gene delivery to aHSCs is a challenging process owing to the stroma-rich microenvironment of a fibrotic liver that restricts the access of nanocarriers to their target cells.[70] Moreover, the hard-to-transfect nature of fibroblast-based aHSCs is a formidable barrier to efficient gene transfer.[71] Furthermore, the vast majority of the reported drug-delivery systems to aHSCs have relied on ligand-

based approaches (*e.g.*, targeting peptides, retinoid derivatives, or antibodies) that exert a negative impact on the *in vivo* stability and pharmacokinetic performance of such systems.[71,72]

We introduced a novel concept for the ligand-free targeting of aHSCs *via* the use of a protein corona-based approach for the gene therapy of liver fibrosis, which is outlined in Fig. 2. To develop this approach, a library of molecularly diverse ionizable lipids was recruited for the delivery of either mRNA or siRNA to aHSCs, both *in vitro* and *in vivo*. A microfluidic device, which is referred to as an invasive lipid nanoparticle production device (iLiNP), was applied to achieve scalable and precise control of the physico-chemical properties of the produced LNPs. Interestingly, the apparent acid dissociation constant (pK_a) of the LNPs was found to play a pivotal role in determining the intrahepatic tropism of the LNPs,[73] where a semi-neutral pK_a (~7.25) favored aHSCs, but an acidic pK_a (5.8–6.7) was more favorable for hepatocytes. Subsequently, two ionizable lipids, CL15A6 and CL15H6, were recognized for their high selectivity to aHSCs. In addition, the particle size of

the LNPs was a key factor in determining the RNA delivery efficiency to aHSCs *in vivo*, where a sub-hundred nm size was essential for an efficient penetration through the stroma barrier of the fibrotic liver, which emphasized the value of recruiting microfluidics technology in the preparation of LNPs that encapsulate RNA therapeutics.[5,51] Moreover, the nitrogen/phosphate (N/P) molar ratio, by which ionizable lipids and RNA are mixed, had a substantial impact on the RNA delivery efficiency. An optimum N/P ratio was required to achieve a balance between the RNA encapsulation efficiency, the endosomal escape capability, and bioavailability of the RNA cargo. Low N/P ratios resulted in poor packaging of the RNA cargo in question, particularly that of mRNA. Furthermore, LNPs with low N/P ratios demonstrated a poor level of functional RNA delivery efficiency, probably because of their low endosomal escape capabilities, which is the critical factor that determines the fate of a nucleic acid payload following the cellular uptake process. High N/P ratios also had a negative impact on the RNA delivery efficiency, owing to the extensive packaging of
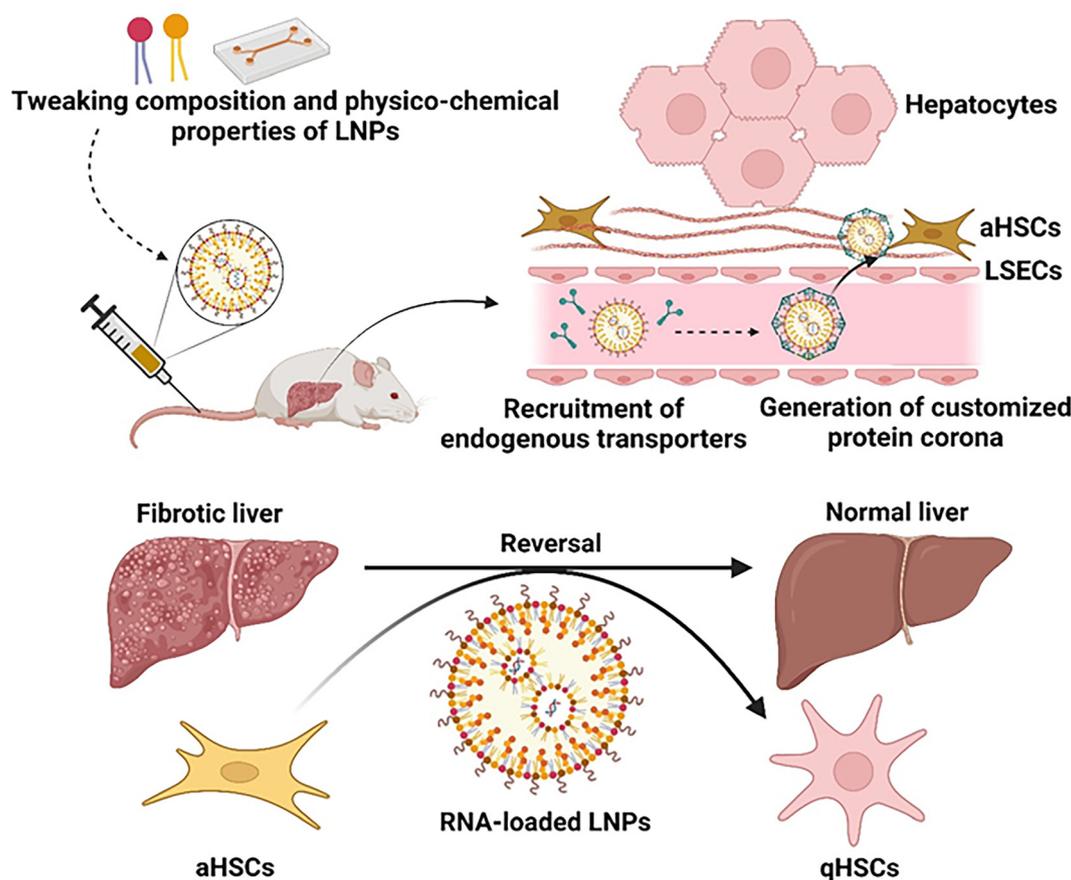
Fig. 2 A schematic of a novel strategy to reprogram aHSCs and reverse liver fibrosis using self-homing LNPs. The composition of LNPs and their physico-chemical properties were tweaked using a combination of ionizable lipids and helper lipids. Following intravenous administration, the LNPs harness endogenous serum proteins to generate a protein corona that houses aHSCs in a fibrotic liver. Tuning the particle size using a microfluidic device allows LNPs to penetrate the stroma-rich microenvironment and access their target. Subsequently, the LNPs deliver a cocktail of siRNAs to reprogram aHSCs into qHSCs and reverse liver fibrosis. The figure is adapted from Younis *et al.*,[5,51] with permission from Elsevier (Copyright 2023, Elsevier).

the anionic RNA, which limits its intracellular release and availability.[74] The results revealed that an N/P ratio of 8–12 is optimum for mRNA delivery to aHSCs. Meanwhile, a lower N/P range of 4–8 is favorable for siRNA delivery. The discrepancies of the optimum parameters between mRNA and siRNA could be attributed to the different molecular size, which affects their packaging into the LNPs and their subsequent intracellular release from them. It is also noteworthy that the mRNA-loaded LNPs had a larger particle size (~80 nm) compared with that of their siRNA-loaded counterparts (~50 nm), which subsequently affects the surface area of LNPs, and potentially affects the nature of the protein corona adsorbed to them.[5,51] Eventually, the helper lipids incorporated into the LNPs dramatically affect their *in vivo* performance. LNPs incorporating phosphoethanol amine derivatives of either 1,2-dioleoyl-*sn*-glycero-3-phosphoethanolamine (DOPE) or 1,2-dipalmitoyl-*sn*-glycero-3-phosphoethanolamine (DPPE) were superior to those with a phosphatidyl choline moiety. This probably could be attributed to their ability to undergo conformational transitions from lamellar to inverted hexagonal orientations, which promotes interactions with the endosomal membrane and subsequently the capability for endosomal escape.[75,76] Interestingly, incorporating phosphatidyl cholines into the LNPs shifted their tropism from aHSCs to hepatocytes, where the unsaturated derivative 1,2-dioleoyl-*sn*-glycero-3-phosphocholine (DOPC) demonstrated a higher efficiency compared with that of the saturated derivative 1,2-distearoyl-*sn*-glycero-3-phosphocholine (DSPC).[51]

Following the systematic optimization described above, self-homing LNPs were generated with high selectivity and efficient RNA delivery to aHSCs. Mechanistic investigations have suggested that such LNPs are delivered to the liver *via* apolipoprotein E (ApoE)-independent machinery, and are potentially recognized by endogenous platelet-derived growth factor (PDGF), which is elevated in the serum in the case of fibrotic diseases. Subsequently, the LNPs are taken up by aHSCs through overexpressed platelet-derived growth factor receptor beta (PDGFRβ) *via* clathrin-mediated endocytosis. The administration of monoclonal antibodies targeting PDGFRβ prior to the administration of LNPs reduced the RNA functional delivery efficiency by approximately 90%, which supports the above hypothesis.[5]

Finally, the abovementioned LNPs were loaded with a cocktail of siRNAs targeting smoothened homologues (SMO) and transforming growth factor beta 1 (TGFβ1) signaling in aHSCs. Therapeutic assessment in mice undergoing thioacetamide (TAA)-induced liver fibrosis revealed a significant reversal of liver fibrosis and restoration of normal liver functions. Analysis of the glioma-associated transcription factors (GLI) suggested the reprogramming of aHSCs into qHSCs by the simultaneous knockdown of Hedgehog (Hh) and TGFβ1 cascades, which are the key pathways involved in the activation of hepatic stellate cells.[77] Meanwhile, single-target monotherapies showed partial amelioration of the fibrotic status, but failed to accomplish the therapeutic goals or restore the healthy status of the liver.[51]

4. Protein corona-mediated extra-hepatic delivery

Extra-hepatic delivery is an important issue in the field of DDS. Tissue-selective delivery using specific ligands is the main strategy, which is based on receptor-mediated endocytosis.[9,10] Recently, there has been increasing research studies regarding tissue-selective delivery without attaching specific ligands, *via* the recruitment of endogenous ligands.[14–16] Such a strategy is considered to be based on the inter-organ trafficking mechanisms in the human body. Herein, we summarize information from the literature on tissue-selective delivery of nanoparticles without the use of specific ligands. In some cases, the endogenous ligands have been clarified. However, in others, no information is available concerning the precise mechanism of tissue-selective delivery and future analysis is required.

4.1 Spleen targeting

Specific and efficient delivery of therapeutic agents such as RNA into the spleen is a key technology for the treatment of a variety of diseases such as cancers, infectious diseases, autoimmune disorders, and all immune-related conditions. The addition of 20–30 mol% of the negatively charged phospholipids that include either phosphatidic acid (PA) or bis(monoacylglycerol)phosphate (BMP) as a fifth lipid component has been used to significantly change the selectivity of LNPs from the liver to the spleen, which is referred to as selective organ targeting (SORT).[78] β2-Glycoprotein I (β2-GPI) is preferentially adsorbed by spleen-tropic LNPs and increases cellular uptake into macrophage cell lines, while apolipoprotein E (ApoE) is most frequently adsorbed by hepatotropic counterparts (Fig. 3).[38] β2-GPI is known to bind phosphatidylserine (PS), which is a negatively charged phospholipid that is exposed as senescent red blood cells promote their clearance by splenic macrophages. This suggests that spleen-targeting SORT LNPs tend to target macrophages. However, further quantitative examination of uptake and gene expression at the cellular level has yet to be conducted. The spleen-targeting SORT LNPs had a lower apparent pK_a that fell between 2 and 6. Kranz *et al.* carefully tuned the charge ratio between mRNA and cationic lipid 1,2-di-*O*-octadecenyl-3-trimethylammonium propane (DOTMA) of an mRNA-lipoplex (RNA-LPX) formulation to achieve a negative net charge. A negatively charged RNA-LPX specifically induced gene expression in the spleen, whereas its cationic counterpart accomplished this in the lungs, as reported elsewhere. Although the mechanism for targeting the spleen was not elucidated, unknown adsorbed proteins could act as endogenous ligands. Furthermore, Luozhong *et al.* reported that the incorporation of 5 mol% PS into DLin-MC3-DMA (MC3)-based mRNA-loaded LNPs dramatically improved gene expression in secondary lymphoid organs such as the spleen and lymph nodes.[79] The expression levels of the PS-LNPs were significantly higher than that of negatively charged phospholipid 1,2-dioleoyl-*sn-glycero*-3-phosphate
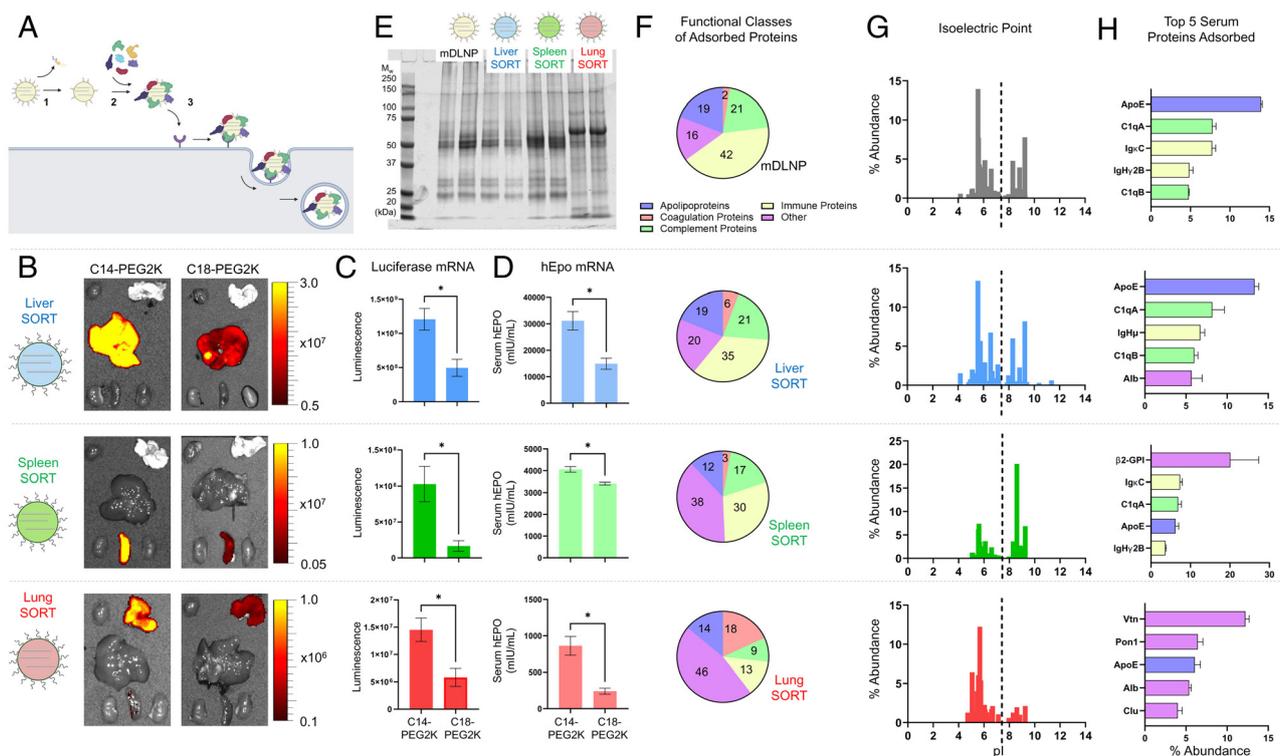
Fig. 3 The mechanism of SORT LNP tissue targeting, including the formation of unique protein coronas. Dilliard *et al.* investigated protein coronas formed on the SORT LNPs. β2-GPI and vitronectin were determined to be the most abundant of proteins, and act as endogenous ligands for target-ing the spleen and lungs, respectively. (A) A proposed three-step endogenous targeting mechanism for tissue-specific mRNA delivery by SORT LNPs in which 1) PEG lipid desorption 2) enables distinct plasma proteins to bind SORT LNPs, 3) resulting in cellular internalization in the target tissues by receptor-mediated uptake. (B) *Ex vivo* bioluminescence of major organs excised from C57BL/6 mice IV injected with liver, spleen, and lung SORT LNPs incorporating either sheddable PEG lipids (C14-PEG$_{2K}$) or less sheddable PEG lipids (C18-PEG$_{2K}$) (0.1 mg FLuc mRNA/kg body weight, 6 h). Total luminescence produced by each organ is reduced when less sheddable PEG lipid is used, suggesting that PEG lipid desorption is a key process for efficacious mRNA delivery by SORT LNPs. (C) Quantification of total luminescence produced by functional protein translated from FLuc mRNA in target organs of C57BL/6 mice IV injected with liver, spleen, and lung SORT LNPs incorporating either C14- or C18-PEG$_{2K}$ (0.1 mg FLuc mRNA/kg body weight, 6 h). (D) ELISA quantification of serum hEPO in C57BL/6 mice treated with liver, spleen, or lung SORT LNPs encapsulating hEPO mRNA (0.1 mg hEPO mRNA/kg body weight, 6 h). Using a less-sheddable PEG reduces SORT LNP potency. (E) SDS−PAGE of the plasma proteins adsorbed to the surface of mDLNP, liver SORT, spleen SORT, and lung SORT LNPs. LNPs with different organ-targeting properties bind distinct plasma pro-teins. (F) The average abundance of proteins with distinct biological functions in the protein coronas of mDLNP and liver, spleen, and lung SORT LNPs. The choice of SORT molecule leads to large-scale differences in the functional ensemble of plasma proteins which bind the LNP. (G) Isoelectric point distribution for the most enriched proteins which constitute 80% of the protein corona of the LNPs. A SORT molecule's headgroup structure influences the pI distribution of the protein corona. (H) The top five most abundant plasma proteins that bind different SORT LNPs (*n* = 3). The chemical structure of SORT molecule affects the number one plasma protein that is most highly enriched on the surface of SORT LNPs. Data are shown as mean ± SEM. Statistical significance was determined using an unpaired two-tailed Student's t test (*P < 0.05). The figure is reproduced from Dilliard *et al.*[143] with permission from Natl. Acad. Sci. USA (Copyright 2021, Natl. Acad. Sci. USA).

(18PA)-incorporated LNPs (consistent with the above-men-tioned spleen-targeting SORT LNPs), suggesting that PS acts as an efficient targeting lipid for secondary lymphoid organs. Although endogenous ligands were not empirically elucidated in this study, it is possible that the aforementioned β2-GPI acts as a ligand to target secondary lymphoid organs.

Based on these results, recent approaches to LNP-based spleen targeting has highly depended on the surface charge, which includes several conditions such as the use of ionizable lipid with a lower apparent pK_a value, the formation of RNA-rich lipoplexes to achieve a negative net charge, and the incor-poration of negatively charged phospholipids. However, an excessive negative charge decreases the functional delivery of

mRNA due to electrostatic interactions with cationically charged lipids, which leads to an inhibition of endosomal escape. Therefore, with the exception of surface charge, an alternative targeting strategy is desirable. Fenton *et al.* suc-ceeded in developing an ionizable lipid, OF-Deg-Lin, that is capable of delivering mRNA into splenic B lymphocytes.[80] Interestingly, intravenous injection of the OF-Deg-Lin LNPs resulted in spleen-specific gene expression, while mainly accumulating in liver tissue. The LNPs were taken up into splenic B lymphocytes at a level consistent with that of splenic monocytes/macrophages. The OF-Deg-Lin LNPs showed an apparent pK_a value of 5.7, which is lower than the typical value suitable for liver targeting. However, detailed targeting mecha-

nisms such as an endogenous ligand/receptor were not elucidated. By contrast, Suzuki *et al.* recently developed an ionizable tri-oleoyl-Tris (iTOT) library. iTOT lipids consist of bulky unsaturated scaffolds similar to that of OF-Deg-Lin, and are more hydrophobic than commercially available ionizable lipids. The authors discovered that increasing the molar ratio of DSPC dramatically suppressed and improved the functional delivery of mRNA in the liver and spleen, respectively. Although this was commonly observed when using both the iTOT and commercially available ionizable lipids, TOT-5, which is one of the iTOT lipids and showed a lower pK_a, achieved maximal spleen-specificity. This suggests a greater level of hydrophobic and near-neutral surface properties, which is important. It is noteworthy that the DSPC-rich formulation resulted in greater levels of both hydrophobicity and microviscosity, which resulted in LNP interface-adsorbed proteins that are more conducive to initiating complement pathways compared with the action of apolipoproteins. As a result, the DSPC-rich LNPs functionally delivered mRNA into splenic B (particularly marginal zone B and MZB) cells *via* the C3b-CD21/35 pathway, which induced MZB-mediated antigen-specific anti-tumor immunity following intravenous injection and enabled the development of safer intramuscularly administered mRNA vaccines.[81,82] In the same context, Younis *et al.* reported that DSPC-rich (20 mol%) LNPs based on an ionizable cationic lipid CL15H6, with a nearly-neutral surface charge, tend to travel to the splenic dendritic cells post-intravenous administration. This creates a potential application as an anticancer vaccine that could demonstrate performance superior to the clinically relevant formulation, RNA-lipoplex, at the same dose.[83] Although the precise mechanism of selectivity remains under investigation, the complement pathway is expected to contribute to the delivery of such LNPs, owing to the presentation of DSPC at the surface of LNPs.[41]

Diverse cell types in the spleen and lymph nodes play different and important roles in the complicated immune cascade, and little is known about target selectivity for diverse cell types. While selective targeting to various immune cell types is important, the formulation of design strategies that focus only on relatively simple properties such as surface charge will face limitations. The discovery of physicochemical properties that could overcome these limitations and the development of novel chemical spaces, as well as advances in high-throughput screening technologies, are highly desirable.

4.2 Lung targeting

The lung is an important organ that is associated with cancer (including metastases from other organs), respiratory infections, and genetic disorders, which makes it an attractive target for mRNA delivery.

Fehring *et al.* have reported on the development of a lung-tropic siRNA-lipoplex (DACC lipoplex) composed of their original cationic lipid AtuFECT01 (β-L-arginyl-2,3-L-diaminopropionic acid-*N*-palmityl-*N*-oleyl-amide trihydrochloride), cholesterol, and mPEG2000-DSPE (1,2-distearoyl-*sn*-glycero-3-phosphoethanol amine-*N* (methoxy (polyethylene glycol)-2000)) at a molar ratio of 70 : 29 : 1.[84] The DACC lipoplex showed a highly cationic property (zeta potential of 40–50 mV). When the DACC lipoplex formulation was used to deliver siRNA to lungs in an injected dose of 40% per gram of lungs, a reduction of greater than 80% in Tie-2 mRNA was documented following consecutive tail vein injections. Improved survival of a lung metastasis model mouse was achieved *via* CD31 inhibition of the lung tissue. An incorporation of 50 mol% of permanently cationic lipid, either 1,2-dioleoyl-3-trimethylammonium-propane (DOTAP), dimethyldioctadecylammonium (DDAB) or 1,2-dimyristoyl-*sn*-glycero-3-ethylphosphocholine (EPC), into ionizable lipid-based LNPs was prepared to deliver mRNA into lungs (referred to as lung-targeting SORT LNPs).[78] The lung-targeting SORT LNPs had a higher (>9) apparent pK_a. Proteomic analysis of a protein corona revealed an enrichment of vitronectin (Vtn) on the lung-targeting SORT LNPs (Fig. 3).[38] Vtn has a RGD motif and is known as an endogenous ligand against $\alpha_v\beta_3$ integrin. Further investigation revealed that variations in the chemical structure of both the hydrophobic scaffold and the hydrophilic headgroup structures impact the quality of functional mRNA delivery to the lungs.[85] The lung-targeting SORT LNPs were able to access lung epithelial cells, which are located in the deeper tissues. This indicates the potential for diverse therapeutic applications such as therapeutic protein expression and genome editing. The lung-selective delivery of mRNA encoding broadly neutralizing antibodies against SARS-CoV-2 variants by utilizing the lung-targeting SORT technology has achieved significant expression of the encoded human monoclonal antibody 8-9D in the lungs and in bronchoalveolar lavage fluid (BALF).[86] Standard liver-tropic LNPs induce high levels of 8-9D antibodies in serum, but have failed to achieve a sufficient concentration of antibodies in BALF. This is because IgG itself lacks the ability to translocate from the bloodstream to mucosal tissues. Importantly, the lung-targeting LNPs exhibited nearly complete protection against beta and Omicron BA.2 strain challenges, whereas their liver-targeting counterparts failed, clearly suggesting the importance of controlled and efficient expression of antibodies in the lungs. As such, the incorporation of permanently cationic lipids into ionizable-based LNPs is a promising strategy for targeting the lungs. However, Omo-Lamai *et al.* reported that the lung-targeting highly cationic LNPs induce massive thrombosis in the lungs and other organs.[87] The thrombosis occurs through the binding of LNPs and changes the confirmation of fibrinogen, activating both platelets and thrombin. The fibrinogen-mediated dangerous clotting could be addressed by pre-treatment/conjugation of the direct thrombin inhibitor bivalirudin and a reduction in the LNP size. Qiu *et al.* discovered that lipidoids with amide bonds (N-series) can achieve lung targeting. However, those with ester bonds (O-series) target the liver.[39] In this system, permanently cationic lipids are not required for lung targeting. Proteomic analysis revealed enrichment of fibrinogen and fibronectin on the N-series LNPs, suggesting these enriched proteins contribute to lung targeting. However, as mentioned above, fibrinogen binding potentially leads to blood clotting.

Indeed, the N-series LNPs increase the plasma levels of thrombin–antithrombin (TAT), which is a marker of recent clotting in the same manner as the lung-targeting SORT LNPs.[87] However, the N-series LNPs achieved induction of genome editing in lungs after co-delivery of Cas9 mRNA and single-guide RNA, which suggests its potential as a radical treatment for lung-related genetic diseases. Xue *et al.* screened combinatorially synthesized cationic degradable lipids for lung targeting *in vivo* utilizing DNA barcoding technology, and identified top-performing lipid CAD9.[88] The LNP-CAD9 exhibited superior functional delivery of Cre mRNA to the lungs compared with the MC3/DOTAP-based SORT LNPs. No information was available in this study regarding either endogenous ligands or apparent pK_a values of the LNP-CAD9.

4.3. Brain targeting

The brain is often considered the most critical organ in the human body due to its extensive range of functions, and its role in essentially every aspect of human life. It acts as the command center for the nervous system and regulates both voluntary and involuntary actions, such as movement, heart rate, and breathing. It is also responsible for higher-order functions such as cognition, emotions, and decision-making, which are essential for learning, memory, and personality. Given its diverse and critical roles, any damage to the brain could significantly impact a person's quality of life, which makes its protection paramount. Thus, the development of brain-targeted therapeutics is gaining increasing attention as a crucial need for improving human health, particularly in the context of an aging global population.[89,90]

Targeting the brain for drug delivery is particularly challenging due to several physiological and biochemical barriers, with the blood–brain barrier (BBB) being the most formidable. Regarding macromolecular brain delivery, innovative therapeutic modalities for various neurodegenerative diseases and brain-related genetic disorders have been developed. These include systemically administered AAV vector, Zolgensma,[91] intrathecal administered antisense oligonucleotides, Nusinersen,[92] the anti-amyloid beta antibody drug, aducanumab,[93] and the transferrin (Tf) receptor-targeted antibody–protein conjugate Pabinafusp Alfa.[94] Strategies using nanoparticles containing LNPs have also been studied, but most of them involve active targeting in which ligand molecules such as antibodies or sugars are presented on the nanoparticle surface.[95,96] These have not been implemented as drugs, and one of the reasons is that the formation of a protein corona inhibits their targeting ability. For example, Tf-conjugated silica nanoparticles bound to serum proteins mask the surface Tf, which reduces the targeting of Tf receptors.[97] Another study reports that polymeric nanoparticles modified with the HIV-1 trans-activating trans-activator peptide and/or alpha neural/glial antigen 2—which are known to cross the blood–brain barrier (BBB) and target oligodendrocyte precursor cells, respectively—are unable to cross the BBB, likely due to the formation of a protein corona.[98] Conversely, the formation of a protein corona is a double-edged sword with respect to target-

ing, and factors that function positively in brain delivery have also been reported. Certain surfactant- or peptide-modified nanoparticles (NPs), such as poly(ethylene glycol)-, polysorbate-, or amyloid β-protein (Aβ)-CN peptide-modified NPs, can absorb apolipoproteins (Apos) like ApoE or ApoB, forming Apo-rich protein coronas. These absorbed proteins interact with lipoprotein receptors on the blood–brain barrier (BBB), thereby facilitating NP entry into the brain.[99–101]

The following is an example of protein corona-mediated brain targeting using systemically administered lipid-based carriers. We also discuss the delivery of small molecules and macromolecules through structural optimization of the constituent lipids, although there is no mention of the impact of a protein corona. One example of protein corona-mediated targeting involves modifying the binding pattern of apolipoproteins on the surface of liposomes, which has been shown to enhance accumulation in the brain and demonstrate therapeutic effectiveness in a mouse model of glioma.[100] This report details how the liposomal surface was altered using a short, non-toxic peptide derived from beta-amyloid ($A\beta_{1–42}$). This modification specifically targets the lipid-binding domain of apolipoproteins to control their adsorption patterns. This engineered liposomal system enables brain-targeting proteins to associate within the bloodstream, effectively exposing their receptor-binding domains on the liposomal surface as they circulate. The second example highlights a study on the lipid derivatization of the neurotransmitter (NT) tryptamine. LNPs containing these lipid derivatives were used for the delivery of small molecules, antisense oligonucleotides (ASO), and proteins to the brain *via* systemic administration.[102] The authors selected three types of NTs—dimethyltryptamine, phenethylamine, and phenylethanolamine—and synthesized NT-derived lipidoids (NT1: dimethyltryptamine, NT2: phenethylamine, NT3: phenylethanolamine). They examined brain accumulation of these lipidoid-incorporated liposome-like nanoparticles using fluorescent labeling, which showed that NT1-lipidoids enhanced brain accumulation more effectively than either NT2- or NT3-lipidoids. NT1-lipidoid nanoparticles combined with various lipids were used to deliver classic polyene antifungal drugs (amphotericin B), tau-ASO, and GFP-Cre fusion proteins to the brain. A possible mechanism of BBB permeation by serotonin receptors and other receptors expressed in brain vascular endothelial cells has been considered, but the details of this mechanism are unknown. Other reports also have screened for brain-targeted LNPs using ionizable lipid libraries conjugated with neuroprotective factors (vinpocetine, berberine) or small molecule ligand structures (L-DOPA, D-serine, temozolomide, tryptamine, cinnamic acid, MK-0752) that are able to pass through the BBB.[103–105] These strategies are distinct in their simplicity of design compared with that of more complicated methods of modifying antibodies and other ligand molecules on the surface of nanoparticles. Furthermore, mRNA is known to be delivered to cerebral vascular endothelial cells without the use of targeting ligands, simply by altering the type and composition of lipids. However, the role of the protein corona is not discussed, and

details of the mechanism remain unknown.[106] The influence of the protein corona on brain delivery and the BBB permeation mechanism are still relatively new research areas, but are being vigorously studied, with future progress expected.[107–109]

4.4. Tumor targeting

"Passive targeting" that relies on the enhanced permeability and retention (EPR) effect to deliver nanoparticles to the tumor tissues has been extensively reported in the literature. Nevertheless, the EPR effect has recently faced a growing number of critics, owing to discrepancies in the tumorous vasculature of experimental animals (mainly mice) and humans, as well as the high levels of inter-patient variability, which have collectively led to the clinical failure of a substantial proportion of the investigated nanotherapeutics.[110] On the other hand, "active targeting" that relies on the attachment of targeting ligands (e.g., peptides, sugars, or antibodies) to the surface of the nanocarriers has encountered several obstacles that hamper its clinical translation, including poor pharmacokinetics, poor ex vivo and in vivo stability, and low scalability, despite promising results in basic research.[11] Therefore, innovative targeting strategies are needed to address the shortcomings of the two aforementioned approaches that have dominated the literature for decades. Herein, the protein corona-based approach provides a promising alternative.[111] A protein corona can exert two-edged roles in the area of tumor targeting. If the protein corona consisted mainly of dysopsonins such as lipoproteins and albumin, this would promote the escape of nanoparticles from the RES and increase the possibility of their tumor accumulation. In addition, some components of the protein corona are recognized by certain receptors on cancerous cells, which thus promotes tumor targeting. On the other hand, if the major components of a protein corona are opsonins (e.g., coagulation proteins, complement, and immunoglobulins), this would reduce the circulation time of the nanoparticles and reduce their chance to reach the tumor tissue. Moreover, the protein corona tends to increase the particle size of nanocarriers, which negatively impacts their ability to extravasate and penetrate tumors.[112]

A classic understanding of active targeting has attributed the mechanism of nanoparticle delivery to the tumor solely to the binding of the targeting ligand to its target receptor on the cancer cells. However, we recently demonstrated a different perspective. Upon decorating an LNP formulation with SP94 peptide, which has a strong selectivity to hepatocellular carcinoma cells (HCC), the LNPs demonstrated a highly selective delivery of siRNA to HCC in vitro.[113] On the contrary, such a formulation failed to induce significant gene silencing in the tumor tissue in vivo. Our systematic optimization revealed that the targeting ligand is not the sole player that affects the in vivo fate of the nanocarriers. Indeed, the composition and physico-chemical properties of the nanocarriers may exert more important roles. In a stroma-rich tumor model like HCC, ultra-small lipid nanoparticles (usLNPs) with an average particle diameter of 60 nm exerted powerful gene silencing activity

in comparison with larger particles, owing to their high capability of penetrating the tumorous microenvironment. In addition, the inclusion of a low ratio of PEG-lipid derivative into usLNPs filled the gaps in the curved surface of the small-sized nanoparticles, which subsequently masked their recognition by apolipoprotein E (ApoE) and reduced their off-target delivery to healthy liver tissues. Furthermore, the ratio of the ionizable lipid and the nature of the helper lipid incorporated into the LNPs had a dramatic impact on their tumor-specific siRNA delivery efficiency.[75]

Another approach in the same context involves the synthesis and screening of huge libraries of molecularly diverse biomaterials, through which the structure–activity relationship (SAR) of such materials could be understood, and materials with intrinsic tumor-homing properties could be identified. Siegwart's group synthesized a library of 1500 biodegradable materials via sequential orthogonal reactions, where biodegradability was imparted through the introduction of metabolically labile ester bonds, and molecular diversity was applied in the cores and peripheries. A candidate, 5A2-SC8, succeeded in achieving a potent siRNA delivery in mice bearing an aggressive MYC-driven HCC model. Moreover, it specifically delivered a tumor-suppressor microRNA, let-7 g, which attenuated tumor growth and improved the survival rate of the mice in question.[114]

Furthermore, functionalization of the nanocarriers with bioinspired or biomimetic materials could generate an "artificial" protein corona that affects their in vivo fate. Huang et al. functionalized nanoparticles with clusterin (Apo J) to serve as an artificial protein corona, which reduced the hepatic and splenic distribution of the nanoparticles and improved their tumor accumulation.[115] In another study, Pan et al. reported that the modification of nanocarriers with bovine serum albumin (BSA) increases their homing to the tumor endothelial cells via the albumin receptor, gp60.[116] Cell-derived coatings have also been investigated. For example, in their natural setting, red blood cells (RBCs) evade RES through the activation of an inhibitory molecule on the surface of macrophages, which is referred to as "signal regulatory protein alpha (SIRPα)". Therefore, functionalization of the nanoparticles with RBC membranes is known to prolong their circulation time by 10-fold compared with the classic PEG coatings.[10,117] Similarly, Zhuang et al. harnessed a platelet membrane coating to selectively deliver siRNA against survivin genes in a mouse model of breast cancer.[118]

4.5. Kidney targeting

The kidney is an important organ for eliminating drugs from the human body, particularly that of small molecular weight compounds. The functional unit of the kidney is a nephron that filters blood to urine via a sieve composed of three layers: an endothelium of glomerular capillaries (70–100 nm), a glomerular basement membrane (GBM: 8–10 nm), and a filtration slit between podocytes (4–30 nm).[119] Therefore, the size of nanoparticles is a critical factor in determining the fate of nanoparticles in the kidney, as summarized in Fig. 4.
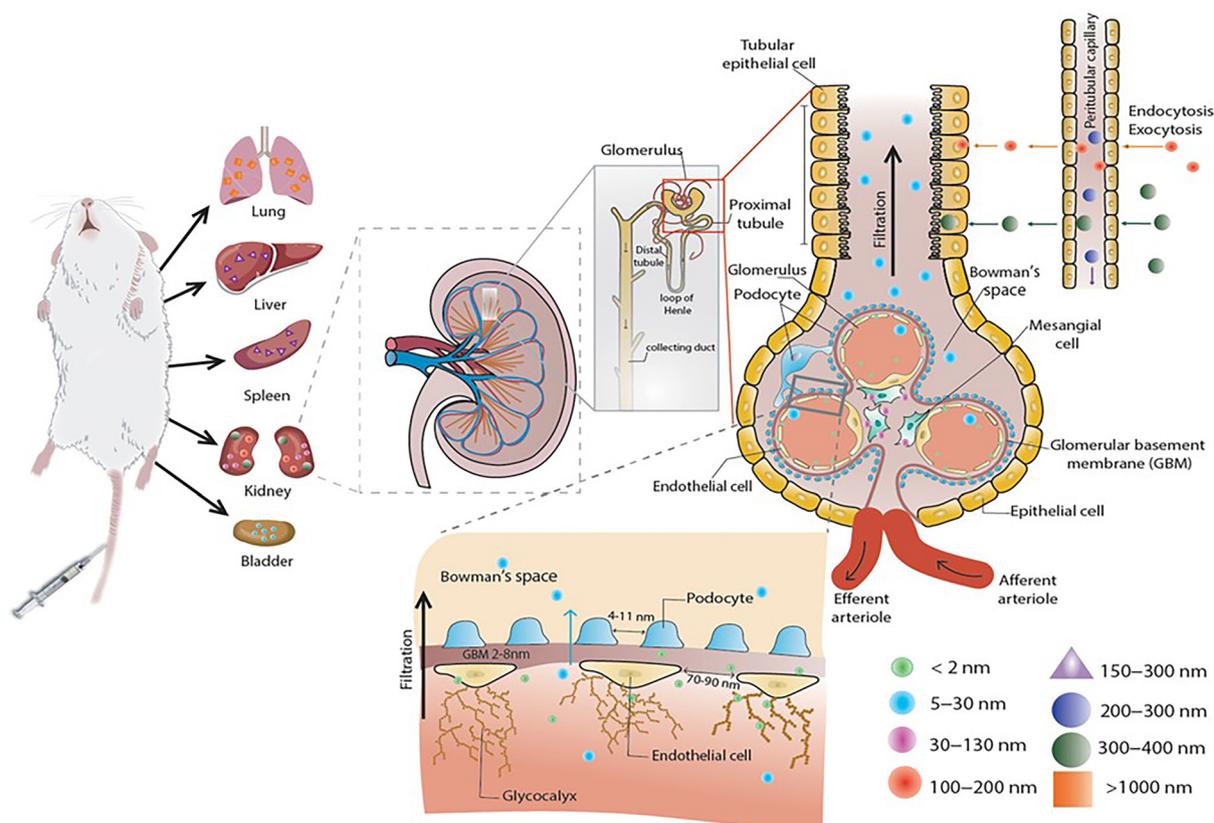
Fig. 4 Impact of the particle size on the distribution of nanoparticles in renal compartments. Nanoparticles smaller than 2 nm are entrapped in endothelial glycocalyx, GBM, and podocytes, while those sized 5–130 nm pass through the glomerular filtration barrier. Smaller nanoparticles (<100 nm) tend to enter the urinary space, whereas larger ones are retained in the mesangium. Glomerular deposition diminishes for nanoparticles >100 nm. Mesoscale nanoparticles (350–400 nm) can enter tubular epithelial cells. Larger nanoparticles (>500 nm) face cellular uptake limitations, and micrometer-scale nanoparticles are trapped in pulmonary capillaries. The figure is reproduced from Cheng et al.,[119] with permission from John Wiley and Sons (Copyright 2024, John Wiley and Sons).

Ultra-small size (<2 nm). Interestingly, ultra-small size nanoparticles (<2 nm) are known to become trapped by the endothelial glycocalyx, the GBM, and podocytes.[120]

Small size (5–30 nm). The smallest nanoparticles are filtered by the glomerulus to the urine. In healthy mice, the cut-off size in glomerular filtration is approximately 10 nm, but this increases up to 30 nm in Adriamycin-damaged kidneys.[121]

Small size (30–130 nm). Size-dependent delivery to mesangial cells has been reported using PEGylated gold nanoparticles between 26 and 167 nm. Transmission electron microscopy has revealed that 75 nm is the optimum size to target mesangial cells in healthy mice.[122] The mesangium is a space outside the capillary lumen that is surrounded by capillaries that are surrounded by GBM, as shown in Fig. 4. Similar size-dependent delivery to mesangial cells was also reported using albumin nanoparticles (ANs) that are between 75 and 130 nm in size, with 95 nm proving to be optimum for the highest rate of delivery to the mesangial cells. All three sizes of ANs should theoretically pass freely through the endothelial fenestrations and enter the mesangium.[123]

Intermediate size (100–200 nm). This size range of nanoparticles cannot be filtered and pass through the glomeruli to reach the peritubular capillaries. However, PEGylated iron oxide cubes/clusters with diameters of 140 nm were excreted in urine via tubular epithelial cells rather than through glomerular filtration. Intravital microscopy analysis has revealed the transportation mechanism: nanoparticles pass through glomeruli to reach the peritubular capillaries, and some of them are endocytosed/exocytosed by endothelial cells to the tubulointerstitium, where they are endocytosed/exocytosed by the proximal tubule epithelial cells.[124] These conditions suggest that endogenous ligands play an important role in endocytic uptake by both peritubular endothelial cells and proximal tubule epithelial cells.

Large size (300–400 nm). Polymeric mesoscale nanoparticles (MNPs) have been examined intensively, and found capable of targeting the tubular epithelium with a 26-fold specificity compared with that of other organs.[125] Di-block polymers poly(lactic-co-glycolic acid) conjugated to polyethyleneglycol with diameters of 300–500 nm were localized in proximal tubular epithelial cells. Researchers believe that MNPs are not filtered by glomerular filtration and reach the peritubular capillaries, whereupon they are transcytosed across the tubular endothelial cells to reach the proximal tubular epithelial cells.[126] Further study is required to prove this transport mechanism, as well as to identify the protein corona that could be the

Table 1 A summary of the reported LNP formulations for the ligand-free extrahepatic delivery of nucleic acids and their physico-chemical properties

Target tissue/cells	Formulation name	Particle size (nm)	PDI	Z-Potential (mV)	pK_a	N/P	EE (%)	Lipid composition	Endogenous ligand/receptor	Physiological condition	Strategy to find	Chemistry	Ref.
Spleen/immune cells	srLNP	66.6 (CryoTEM)	—	−22	—	6	93	MC3:DSPG:Chol:DMG-PEG$_{2K}$ (50:10:38.5:1.5 mol%)	Stabilin-2 (receptor)	Healthy	Replacing neutral phospholipids with anionic phospholipids	Ionizable lipid and anionic phospholipid	44
	CL15F6-4 LNP	229.3	0.316	−5.87	6.9	6	66.7	CL15F6-4:DSPC:Chol:DMG-PEG$_{2K}$ (50:10:38.5:1.5 mol%)	Not determined	Healthy	Systematic examination of the tail structure of ionizable lipids	Ionizable lipids with branched tails of different total carbon length	144
	A-11-LNP	547	0.19	−1.4	—	7.2	89.2	CL4H6:DOPE:Chol:DSG-PEG$_{2K}$ (60:10:30:1.5 mol%)	Not determined	Healthy	Formulation optimization by DoE	Ionizable lipid	145
	RNA-LPX	~270	~0.24	~−32	—	0.65	~80	DOTMA:DOPE (50:50 mol%)	Not determined	Healthy	Optimization of the mRNA/lipid charge ratio	Cationic lipid	62
	Spleen SORT	167.8	0.144	−1.84	3.97	—	—	5A2-SC8:DOPE:Chol:DMG-PEG$_{2K}$:18PA (16.7:16.7:33.3:3.3:30 mol%)	β2-GPI	Healthy	Systematic examination of the fifth lipid component	Ionizable lipid and anionic phospholipid	143
	PS-LNP	95.46	0.132	−2.58	6.31	6	>85	MC3:DSPC:Chol:DMG-PEG$_{2K}$:DOPS (50:10:38.5:1.5:5 mol%)	Not determined	Healthy	Biomimetic use of PS that recognized by phagocytes	Ionizable lipid and PS derivative	146
	OF-Deg-Lin LNPs	75	0.197	—	5.7	—	59	OF-Deg-Lin:DOPE:Chol:DMG-PEG$_{2K}$ (35:16:46.5:2.5 mol%)	C3b-CD21/35 (receptor)	Healthy	—	Ionizable lipid with degradable linkages	80
	15% DSPC LNP	109	0.11	1.8	6.2	10.2	90.3	TOT-5:DSPC:Chol:DMG-PEG$_{2K}$ (65:15:20:1.5 mol%)	C3b-CD21/35 (receptor)	Healthy	Increase in the hydrophobicity and microviscosity of the LNP interface	Ionizable lipid and helper phospholipid	82
	CL15H6 LNPs	~80	<0.1	−0.5 – (2.4)	7.25	8	>90	CL15H6:DSPC:Chol:DMG-PEG$_{2K}$ (60:20:20:3 mol%)	Not determined	Healthy	Step-wise formulation optimization	Ionizable lipid and helper phospholipid	83
Lung	DACC lipoplex	74	0.25–0.35	46.4	—	8.4	—	AtuFECT01:Chol:DSPE-PEG$_{2K}$ (70:29:1 mol%)	Not determined	Healthy	In vivo screening of biodistribution	Cationic lipid	84
	Lung SORT	114.8	0.159	−0.89	>11	—	—	5A2-SC8:DOPE:Chol:DMG-PEG$_{2K}$:DOTAP (11.9:11.9:23.8:2.4:50 mol%)	Vitronectin	Healthy	Systematic examination of the fifth lipid component	Permanently-cationic lipid	143
	306-N16 LNP	81	0.2	−5	—	—	—	306-N16:Chol:DOPC:DMG-PEG$_{2K}$ (50:38.5:10:1.5 mol%)	Fibrinogen	Healthy	Examination of the impact of linker chemistry on organ targeting	Lipidoid with an amide linker in hydrophobic tails (N-series)	147
Brain	LNP-CAD9	150.1	0.21	4.5	—	—	—	3-A2-7b:DOPE:Chol:DMG-PEG$_{2K}$ (35:16:46.5:2.5 mol%)	Not determined	Healthy	In vivo screening via DNA barcoding	Combinatorial cationic degradable (CAD) lipid	148
	SLN (cetyl palmitate NP)	211.3	—	−10	—	—	—	Cetyl palmitate, polysorbate 80	Artificial ApoE4 corona	Healthy	Protein corona decoration (ApoE4 adsorption)	Cetyl palmitate (C16) solid core stabilized by polysorbate 80 surfactant	99
	sLip/SP-sLip	152	0.06	−39.5	—	—	—	HSPC:Chol:mPEG2000-DSPE/SP-PEG3400-DSPE (52:43:3:2 mol%)	ApoE, ApoA1, ApoJ	Intracranial glioblastoma (U87) in mice	Rational design (brain-targeting peptide to recruit ApoE)	Peptide (SP) on PEG-DSPE, HSPC	100
	PTX loaded Aβ-CN-PMs (PTX/Aβ-CN-PMs)	103.1	0.184	7.23	—	—	90.3	20 mg of mPEG2000-PLA1300, 1.8 mg of Aβ-CN-PEG2000-PLA1300, and 2 mg of PTX	ApoE (enriched corona via Aβ peptide)	Orthotopic U87 glioma in mice	Rational design (Aβ peptide for ApoE adsorption)	PEG-PLA polymer with an Aβ peptide graft	101

© 2025 The Author(s). Published by the Royal Society of Chemistry

Table 1 (Contd.)

Target tissue/cells	Formulation name	Particle size (nm)	PDI	Z-Potential (mV)	pKa	N/P	EE (%)	Lipid composition	Endogenous ligand/receptor	Physiological condition	Strategy to find	Chemistry	Ref.
	NT1 (tryptamine)-derived lipidoid LNPs	100–800 (AmB-loaded LNP), 150–160 (ASO-loaded LNP), 100–250 (GFP-Cre loaded LNP)	0.2–0.4 (AmB-loaded LNP), 0.2 (ASO-loaded LNP)	20–30 (AmB-loaded LNP), −18 (ASO-loaded LNP)	—	—	—	NT1-O12B:PBA-Q76-O16B (AmB-loaded LNP), NT1-O14B:306-O12B-3:DSPE-PEG$_{2K}$ (ASO-loaded LNP), NT1-O14B:PBA-Q76-O16B (GFP-Cre-loaded LNP)	Not determined	Healthy	Rational design (neurotransmitter-derived lipidoid)	Tryptamine-derived ionizable lipid (NT1)	102
	Vinpocetine-derived ionizable lipidoid LNPs	93.7	0.167	1.7	6.2–6.5	—	91.1	A5-B1-C4.2:DOPC:Chol:DMG-PEG$_{2K}$ (50:12.5:36:1.5 mol%)	Not determined	Healthy/AD model mice	Library screening (structure–activity for BBB and CBF)	Cyclic tertiary amine (vincamine derivative)	103
	Berberine-inspired ionizable lipid LNPs	63.94	0.201	−7	6.0–7.0	—	—	A2-B13:DOPC:Chol:DMG-PEG$_{2K}$ (39:30:30:1 mol%)	Not determined	Healthy/APP/PS1 mice	Library screening (alkaloid scaffold)	Tetrahydroisoquinoline (protoberberine)	104
	MK16 BLNPs	125	0.125	6	6.86	BL/mRNA = 12.5/1	80	MK16:DOPE:Chol:DMG-PEG$_{2K}$ (60:30:40:0.75 mol%)	Not determined	Healthy/disease	Combinatorial screening (BLNP library)	Proprietary ionizable lipid scaffold	105
	Cat-LNP	76	0.13	(Cationic)	~6	~3/1	96	cKK-E12 (51.4%):Chol (38.6%):C14-PEG$_{2K}$ (10%)	Not determined	Healthy	Rational design (cationic helper lipid)	Pyridazine-based cationic lipid (cKK-E12)	106
Tumor	5A2-SC8	64	—	−0.74	6.59	—	>90	5A2-SC8:DSPC:Chol:lipid-PEG$_{2K}$ (50:38:10:2 mol%)	Not determined	HCC	High throughput screening of a huge library (1500 compounds)	Modular degradable dendrimers	114
	DODAP LNPs	~80	~0.2	−1.6	~6.5	6	>90	DODAP:DOPE:Chol:DMG-PEG$_{2K}$ (50:30:20:3 mol%)	Not determined	Breast cancer	Formulation screening and optimization	Ionizable lipid and helper phospholipid	149
Kidney	Polymeric mesoscale NPs	386.7 (A-MNP), 402.8 (C-MNP)	—	−19.5 (A-MNP), 18.3 (C-MNP)	—	—	—	PEG/PLGA	Not determined	Healthy	Random	Poly(lactic-co-glycolic acid) conjugated to polyethylene glycol	150
Placenta	LNP55	122	0.265	3.81	5.92/5.76 (pipette/microfluidic)	—	79.4	C14-494:DOPE:Chol:DMG-PEG$_{2K}$ (35:24:46.5:2.5 mol%)	β2-GPI	Pre-eclampsia	In vivo screening via DNA barcoding	Ionizable lipid	133
Pancreas	Lipidoid LNP	173.9	0.138	—	6.4	—	89.3	Lipidoid 306Oi$_{10}$:DOTAP:Chol:PEG-lipid (35:40:22.5:2.5 mol%)	Not determined	Healthy	Formulation screening and optimization	Branched ionizable cationic lipid	137
	Pantgt LNP	167–208	0.12–00.31	(−2)–(−5)	7.17–8.34	—	~80	P6CIT:Chol:DSPC:DMG-PEG$_{2K}$ (16:8:8:3 mass ratio)	Not determined	Pancreatic cancer	Formulation optimization by DoE	Polyethyleneimine (PEI)-based cationic lipid	138
Bone marrow	BM1	45.2	0.19	—	6.55	—	—	7C1:Chol:C18PEG 2000 (80:2.5:17.5 mol%)	Not determined	Healthy	In vivo screening via DNA barcoding	Ionizable lipid and long-chained PEG-lipid	140

Abbreviations: EE, encapsulation efficiency; DSPG, 1,2-distearoyl-*sn*-glycero-3-phosphoglycerol; Chol, cholesterol; DMG-PEG$_{2K}$, 1,2-dimyristoyl-*rac*-glycero-3-methoxypolyethylene glycol-2000; DSG-PEG 2000, distearoyl-*rac*-glycerol-PEG 2000; DoE, design of experiments; DOTMA, 1,2-di-O-octadecenyl-3-trimethylammonium propane; DOPE, 1,2-dioleoyl-*sn*-glycero-3-phosphoethanolamine; 18PA, 1,2-distearoyl-*sn*-glycero-3-phosphate; DSPC, 1,2-distearoyl-*sn*-glycero-3-phosphocholine; DOPS, 1,2-di-(9Z-octadecenoyl)-*sn*-glycero-3-phospho-L-serine; PS, phosphatidyl serine; DSPE-PEG 2000, 1,2-distearoyl-*sn*-glycero-3-phosphoethanolamine-N-[amino (polyethylene glycol)-2000]; DOPC, 1,2-dioleoyl-*sn*-glycero-3-phosphocholine; HCC, hepatocellular carcinoma; DODAP, 1,2-dioleoyl-3-dimethylammonium-propane.

cause of this surprising mechanism. Han *et al.* synthesized triptolide-loaded mesoscale polydopamine melanin-mimetic nanoparticles (MeNP$^{TP}_4$) as both an antioxidant and an anti-inflammatory therapeutic platform to synergistically scavenge reactive oxygen/nitrogen species, and inhibit the activity of macrophages and dendritic cells to generate Treg cells for acute kidney injury therapy.[127] The underlying mechanisms that target kidneys without using a specific ligand should be clarified in the near future. This phenomenon, however, could also be further evidence for protein corona-mediated active targeting.

The surface charge of nanoparticles is also an important parameter in glomerular filtration. The filtration barrier has a strong negative charge from heparan sulfate in the glycocalyx and anionic proteoglycans on the GBM. These exert a strong repulsive force on the negatively charged particles, which prevents the glomerular passage of negatively charged particles.[128]

Shape is another important factor that helps determine the efficiency of glomerular filtration.[128] Disk or rod-like nanoparticles have longer circulation times compared with that of spherical nanoparticles because it is easier for macrophages to internalize spherical shapes due to the higher probability of interactions with the high curvature of membranes. Single-walled carbon nanotubes with a molecular weight of ~350–500 kDa, a length of 100–500 nm, and a diameter of 1.2 nm were found to be similarly cleared *via* glomerular filtration.[129] As long as nanoparticle width is below the size cutoff (~10 nm), different lengths follow an order of magnitude for clearance *via* glomerular filtration.

4.6. Placenta targeting

The placenta is considered an important organ from the viewpoint of mRNA medicine, since pre-eclampsia affects 3–5% of all pregnancies and is a leading cause of maternal and fetal morbidity.[130] Although mRNA delivery of VEGF *via* viral vectors has shown positive results in preclinical studies, there are serious problems to be solved before clinical translations, such as immunogenicity, non-specific delivery and packaging, and manufacturing limitations can be resolved.[130] Several studies have been reported on LNP as an expected technology, where they used a strategy of two-stage screening from *in vitro* screening to *in vivo* optimization.[131,132] Recently, a new strategy of *in vivo* screening using DNA barcodes (b-DNA) without the need for *in vitro* screening has been reported.[133] The authors proposed endogenous ligand-mediated delivery to the placenta. A library of ionizable lipids was synthesized *via* an S_N2 reaction between epoxide tails (C12/14/16) and eight polyamine cores. This 98-LNP library of 24 ionizable lipids was constructed by changing lipid formulations, including C12-200 and DLin-MC3-DMA as liver-tropic LNP references. In two models of pre-eclampsia induced by inflammation or hypoxia, LNP55 encapsulating mRNA of VEGF cured maternal hypertension and fetal health, and improved the serum level of the clinical biomarker-soluble Fms-like tyrosine kinase-1. β_2-

Glycoprotein I (β_2-GPI) is suggested as an endogenous ligand for placenta-targeting LNP55.[133]

4.7. Pancreas targeting

The pancreas is a small visceral secretory gland that plays vital roles in digestion and metabolism, particularly through the secretion of insulin and glucagon hormones that regulate the blood glucose level. Subsequently, targeting the pancreas holds promise for the treatment of various metabolic disorders, such as diabetes mellitus and obesity.[134] In addition, pancreatic cancer is one of the most aggressive life-terminating cancers.[135] Despite its clinical significance, there have been very few studies in the literature targeting the pancreas, probably because of the difficulty in achieving selective drug delivery to it through non-invasive routes.[136]

In an interesting recent study, Whitehead's group reported a successful strategy for the selective delivery of mRNA to the insulin-producing pancreatic β cells *via* the use of intra-peritoneally (IP)-administered LNPs. These LNPs were formulated using a combination of structurally diverse ionizable lipids (lipidoids) and helper lipids, where the incorporation of a cationic helper lipid, DOTAP, improved the efficiency of mRNA delivery to the pancreas. Interestingly, mechanistic investigations suggested that LNPs were first taken up by peritoneal macrophages, which subsequently facilitate the pancreatic delivery of mRNA through an exosome-mediated horizontal gene transfer.[137]

In another study, Shen and co-workers reported on the delivery of interleukin-12 (IL-12)-encoding mRNA to an orthotopic model of pancreatic ductal adenocarcinoma following the IP administration of LNPs based on a cationic lipid, P6CIT, and a mixture of cholesterol, DSPC, and DMG-PEG 2000 as helper lipids. The composition of LNPs was optimized using the Design-of-Experiments (DoE) approach. The developed therapy succeeded in the immunological reprogramming of the tumor microenvironment from a "cold" to a "hot" microenvironment, with a subsequent efficient eradication of the tumor.[138] Although the precise mechanism of the LNP delivery to the spleen was not revealed in this study, peritoneal macrophages could have played a role in mediating such a delivery, in a manner similar to that of the above-mentioned study.

4.8. Bone marrow targeting

While many previous studies have reported the targeting of endothelial cells in livers and lungs using LNPs, targeting bone marrow endothelial cells (BMECs) has been considered unreachable through systemic administration. BMECs modulate the signaling of pericytes, immune cells, and hematopoietic stem cells. Therefore, they offer an interesting target for the treatment of hearth diseases, blood disorders, and many of the effects of aging.[139]

Dahlman's group applied the concept of protein corona-based targeting to deliver either siRNA for gene silencing or single-guide RNA (sgRNA) for genome editing to BMECs post systemic administration. A barcoding strategy was introduced, in which LNPs were labelled with specific short DNA barcodes

to enable high-throughput screening of more than 100 LNPs in a single mouse. Subsequently, next-generation sequencing (NGS) was used to track the *in vivo* fate of the administered LNPs. Through an *in vivo*-directed evolution strategy, an enriched LNP (referred to as BM1) was identified. BM1 had a simple composition of an ionizable lipid, 7C1, cholesterol, and C18PEG$_{2K}$. Interestingly, the particle size of LNPs did not affect their *in vivo* tropism. By contrast, the chemical composition of LNPs, mainly the cholesterol ratio and the length of the PEG-lipid tail, had a dramatic impact on the *in vivo* tropism toward BMECs. The authors hypothesized that the selectivity to BMECs could have been attributed to a combination of two potential factors. First, the length of the PEG-lipid tail could have affected the pharmacokinetics of LNPs and shielded them from the reticulo-endothelial system (RES), with a subsequent escape from hepatic and splenic accumulations. Second, the introduction of cholesterol could have affected the binding of serum proteins to the surface of LNPs, which subsequently would have affected the composition of the formed protein corona.[140]

5. Conclusions and perspectives

During the COVID-19 pandemic, LNP technology contributed significantly to the development of mRNA vaccines, which saved the whole world. The next step of LNP technology is to expand the therapeutic area from liver hepatocytes to other tissues/cells in our body. Active targeting has been developed based on specific receptor-mediated endocytosis *via* introducing specific ligands on the surface of nanoparticles. However, a clinically established active targeting system has not been achieved, although there are many successful reports of pre-clinical situations. As described above, the *in vivo* biodistribution of nanoparticles is influenced remarkably by the composition and properties of the nanocarrier, although underlying mechanisms are not precisely identified yet. Therefore, there is increasing information regarding the potential impact of protein corona on the tissue distribution of nanoparticles. However, it is still analytically difficult to identify an endogenous ligand, which enhances biodistribution to a specific tissue. In this literature review, we attempted to gather the available information on the reported LNP formulations for ligand-free delivery of nucleic acids to a wide variety of extrahepatic tissues and cell populations, extracting their physicochemical properties, and trying to correlate such properties with their *in vivo* tropism. The information is summarized in Table 1.

Although ligand-based active targeting relies on a concrete knowledge of specific pathways and receptors, making it more reliable from the theoretical point of view, the clinical translation of such delivery systems is hampered by their low stability, complexity, and scalability issues.[11] On the other hand, protein corona-based targeting simplifies the composition and production of nanoparticles, which can address the above challenges and contribute to the improvement of the clinical

translatability of nanomedicines. Nevertheless, there are still multiple challenges that encounter such a promising approach, including the inter-subject variability in the levels of the endogenous ligands in question as well as their alterations depending on the physiological and pathological conditions, which subtracts from the reproducibility of the developed delivery systems.[141] In addition, the limited precise information on the interactions between such delivery systems and the endogenous macromolecules and their physiological consequences raises some concerns on the biosafety of this emerging technology, and complicates its adoption from a regulatory point of view.[142]

In the present article, we highlighted a successful delivery system to activated hepatic stellate cells in fibrotic liver, which has been developed based on screening a library of ionizable cationic lipids with an intensive optimization of LNP formulation. This strategy can be extended to other tissues/cells to find a protein corona-mediated selective system to the spleen, the lungs, the brain, tumors, kidneys, *etc*. In the human body, there are well organized network systems *via* blood circulation for the cell-to-cell transport of macromolecules such as hormones (insulin, growth factors), lipid particles (HDL, LDL), and exosomes. We believe that by the end of the 21st century, researchers will have harnessed the power of the endogenous mechanisms of the human body for trafficking to achieve the highest possible level of drug targeting.

Author contributions

M. Y., S. K., Y. S. and H. H. conceived, designed, reviewed and edited the manuscript. H. H. wrote the abstract and sections 4.5, 4.6 and 5; Y. S. wrote sections 2, 4.1 and 4.2; M. Y. wrote section 1, 3, 4.4, 4.7, 4.8, and 5. S. K. wrote section 4.3. H. H. supervised all the writing of the manuscript and acquired funding.

Conflicts of interest

The authors declare that they have no competing interests.

Data availability

No primary research results, software or code has been included and no new data were generated or analyzed as part of this review.

Acknowledgements

Education, Culture, Sports, Science and Technology (MEXT) (HH). We appreciate the helpful advice from Dr James McDonald in the language review of this manuscript.

References

1 A. Akinc, M. A. Maier, M. Manoharan, K. Fitzgerald, M. Jayaraman, S. Barros, S. Ansell, X. Du, M. J. Hope, T. D. Madden, B. L. Mui, S. C. Semple, Y. K. Tam, M. Ciufolini, D. Witzigmann, J. A. Kulkarni, R. van der Meel and P. R. Cullis, *Nat. Nanotechnol.*, 2019, **14**, 1084–1087.

2 F. P. Polack, S. J. Thomas, N. Kitchin, J. Absalon, A. Gurtman, S. Lockhart, J. L. Perez, G. Pérez Marc, E. D. Moreira, C. Zerbini, R. Bailey, K. A. Swanson, S. Roychoudhury, K. Koury, P. Li, W. V. Kalina, D. Cooper, R. W. Frenck Jr., L. L. Hammitt, Ö. Türeci, H. Nell, A. Schaefer, S. Ünal, D. B. Tresnan, S. Mather, P. R. Dormitzer, U. Şahin, K. U. Jansen and W. C. Gruber, *N. Engl. J. Med.*, 2020, **383**, 2603–2615.

3 X. Cheng and R. J. Lee, *Adv. Drug Delivery Rev.*, 2016, **99**, 129–137.

4 S. Kimura and H. Harashima, *J. Controlled Release*, 2023, **362**, 797–811.

5 M. A. Younis, Y. Sato, Y. H. A. Elewa, Y. Kon and H. Harashima, *J. Controlled Release*, 2023, **353**, 685–698.

6 J. Nong, P. M. Glassman and V. R. Muzykantov, *Adv. Drug Delivery Rev.*, 2022, **184**, 114180.

7 X. Cong, Z. Zhang, H. Li, Y.-G. Yang, Y. Zhang and T. Sun, *J. Nanobiotechnol.*, 2024, **22**, 620.

8 Y. Feng, Q. Tang, B. Wang, Q. Yang, Y. Zhang, L. Lei and S. Li, *J. Nanobiotechnol.*, 2024, **22**, 737.

9 Y. Sato, Y. Sakurai, K. Kajimoto, T. Nakamura, Y. Yamada, H. Akita and H. Harashima, *Macromol. Biosci.*, 2017, **17**, 1600179.

10 T. Nakamura, Y. Sato, Y. Yamada, M. M. Abd Elwakil, S. Kimura, M. A. Younis and H. Harashima, *Adv. Drug Delivery Rev.*, 2022, **188**, 114417.

11 M. A. Younis, H. M. Tawfeek, A. A. H. Abdellatif, J. A. Abdel-Aleem and H. Harashima, *Adv. Drug Delivery Rev.*, 2022, **181**, 114083.

12 S. Wang, J. Zhang, H. Zhou, Y. C. Lu, X. Jin, L. Luo and J. You, *J. Controlled Release*, 2023, **360**, 15–43.

13 M. J. Hajipour, R. Safavi-Sohi, S. Sharifi, N. Mahmoud, A. A. Ashkarran, E. Voke, V. Serpooshan, M. Ramezankhani, A. S. Milani, M. P. Landry and M. Mahmoudi, *Small*, 2023, **19**, e2301838.

14 W. C. Chou and Z. Lin, *Curr. Opin. Biotechnol*, 2024, **85**, 103046.

15 L. Fu, Y. Zhang, R. A. Farokhzad, B. B. Mendes, J. Conde and J. Shi, *Chem. Soc. Rev.*, 2023, **52**, 7579–7601.

16 M. Yuan, Z. Han, Y. Liang, Y. Sun, B. He, W. Chen and F. Li, *Biomater. Res.*, 2023, **27**, 90.

17 G. Caracciolo, *Nanoscale*, 2018, **10**, 4167–4172.

18 S. Schöttler, G. Becker, S. Winzen, T. Steinbach, K. Mohr, K. Landfester, V. Mailänder and F. R. Wurm, *Nat. Nanotechnol.*, 2016, **11**, 372–377.

19 W.-C. Chou and Z. Lin, *Curr. Opin. Biotechnol.*, 2024, **85**, 103046.

20 M. Jansch, P. Stumpf, C. Graf, E. Rühl and R. H. Müller, *Int. J. Pharm.*, 2012, **428**, 125–133.

21 S. Palchetti, V. Colapicchioni, L. Digiacomo, G. Caracciolo, D. Pozzi, A. L. Capriotti, G. La Barbera and A. Laganà, *Biochim. Biophys. Acta*, 2016, **1858**, 189–196.

22 D. Pozzi, G. Caracciolo, L. Digiacomo, V. Colapicchioni, S. Palchetti, A. L. Capriotti, C. Cavaliere, R. Zenezini Chiozzi, A. Puglisi and A. Laganà, *Nanoscale*, 2015, **7**, 13958–13966.

23 J. Simon, G. Kuhn, M. Fichter, S. Gehring, K. Landfester and V. Mailänder, *Cells*, 2021, **10**, 132.

24 M. Lundqvist, C. Augustsson, M. Lilja, K. Lundkvist, B. Dahlbäck, S. Linse and T. Cedervall, *PLoS One*, 2017, **12**, e0175871.

25 S. Schöttler, K. Klein, K. Landfester and V. Mailänder, *Nanoscale*, 2016, **8**, 5526–5536.

26 M. J. Hajipour, S. Laurent, A. Aghaie, F. Rezaee and M. Mahmoudi, *Biomater. Sci.*, 2014, **2**, 1210–1221.

27 K. S. Kelly-Spratt, S. J. Pitteri, K. E. Gurley, D. Liggitt, A. Chin, J. Kennedy, C.-H. Wong, Q. Zhang, T. B. Buson, H. Wang, S. M. Hanash and C. J. Kemp, *PLoS One*, 2011, **6**, e19721.

28 U. Sakulkhu, M. Mahmoudi, L. Maurizi, J. Salaklang and H. Hofmann, *Sci. Rep.*, 2014, **4**, 5020.

29 G. Caracciolo, R. Safavi-Sohi, R. Malekzadeh, H. Poustchi, M. Vasighi, R. Zenezini Chiozzi, A. L. Capriotti, A. Laganà, M. Hajipour, M. Di Domenico, A. Di Carlo, D. Caputo, H. Aghaverdi, M. Papi, V. Palmieri, A. Santoni, S. Palchetti, L. Digiacomo, D. Pozzi, K. S. Suslick and M. Mahmoudi, *Nanoscale Horiz.*, 2019, **4**, 1063–1076.

30 J. Szebeni, B. Kiss, T. Bozó, K. Turjeman, Y. Levi-Kalisman, Y. Barenholz and M. Kellermayer, *ACS Nano*, 2023, **17**, 13147–13157.

31 A. Henrickson, J. A. Kulkarni, J. Zaifman, G. E. Gorbet, P. R. Cullis and B. Demeler, *ACS Nano*, 2021, **15**, 5068–5076.

32 V. Francia, R. M. Schiffelers, P. R. Cullis and D. Witzigmann, *Bioconjugate Chem.*, 2020, **31**, 2046–2059.

33 Y. C. Hacene, A. Loiseau, V. D. P. Maio, P. Grenier, E. Boisselier and N. Bertrand, *Nano Lett.*, 2021, **21**, 4530–4538.

34 K. Liu, R. Nilsson, E. Lázaro-Ibáñez, H. Duàn, T. Miliotis, M. Strimfors, M. Lerche, A. R. Salgado Ribeiro, J. Ulander, D. Lindén, A. Salvati and A. Sabirsh, *Nat. Commun.*, 2023, **14**, 4007.

35 V. Francia, Y. Zhang, M. H. Y. Cheng, R. M. Schiffelers, D. Witzigmann and P. R. Cullis, *Proc. Natl. Acad. Sci. U. S. A.*, 2024, **121**, e2307803120.

36 D. Baimanov, J. Wang, Y. Liu, P. Zheng, S. Yu, F. Liu, D. Boraschi, Y. Zhao, C. Chen and L. Wang, *J. Am. Chem. Soc.*, 2025, **147**, 7604–7616.

37 L. Miao, J. Lin, Y. Huang, L. Li, D. Delcassian, Y. Ge, Y. Shi and D. G. Anderson, *Nat. Commun.*, 2020, **11**, 2424.

38 S. A. Dilliard, Q. Cheng and D. J. Siegwart, *Proc. Natl. Acad. Sci. U. S. A.*, 2021, **118**, e2109256118.

39 M. Qiu, Y. Tang, J. Chen, R. Muriph, Z. Ye, C. Huang, J. Evans, E. P. Henske and Q. Xu, *Proc. Natl. Acad. Sci. U. S. A.*, 2022, **119**, e2116271119.

40 H. Gharibi, A. A. Ashkarran, M. Jafari, E. Voke, M. P. Landry, A. A. Saei and M. Mahmoudi, *Nat. Commun.*, 2024, **15**, 342.

41 M. Yanez Arteta, T. Kjellman, S. Bartesaghi, S. Wallin, X. Wu, A. J. Kvist, A. Dabkowska, N. Székely, A. Radulescu, J. Bergenholtz and L. Lindfors, *Proc. Natl. Acad. Sci. U. S. A.*, 2018, **115**, E3351–E3360.

42 N. Chander, G. Basha, M. H. Yan Cheng, D. Witzigmann and P. R. Cullis, *Mol. Ther. – Methods Clin. Dev.*, 2023, **30**, 235–245.

43 A. Hashiba, M. Toyooka, Y. Sato, M. Maeki, M. Tokeshi and H. Harashima, *J. Controlled Release*, 2020, **327**, 467–476.

44 R. Pattipeiluhu, G. Arias-Alpizar, G. Basha, K. Y. T. Chan, J. Bussmann, T. H. Sharp, M. A. Moradi, N. Sommerdijk, E. N. Harris, P. R. Cullis, A. Kros, D. Witzigmann and F. Campbell, *Adv. Mater.*, 2022, **34**, e2201095.

45 Z. Li, J. Carter, L. Santos, C. Webster, C. F. van der Walle, P. Li, S. E. Rogers and J. R. Lu, *ACS Nano*, 2023, **17**, 979–990.

46 Y. Fei, X. Yu, P. Liu, H. Ren, T. Wei and Q. Cheng, *Adv. Mater.*, 2024, **36**, e2409812.

47 Y. Sato, Y. Note, M. Maeki, N. Kaji, Y. Baba, M. Tokeshi and H. Harashima, *J. Controlled Release*, 2016, **229**, 48–57.

48 Y. Sato, K. Hashiba, K. Sasaki, M. Maeki, M. Tokeshi and H. Harashima, *J. Controlled Release*, 2019, **295**, 140–152.

49 M. Jayaraman, S. M. Ansell, B. L. Mui, Y. K. Tam, J. Chen, X. Du, D. Butler, L. Eltepu, S. Matsuda, J. K. Narayanannair, K. G. Rajeev, I. M. Hafez, A. Akinc, M. A. Maier, M. A. Tracy, P. R. Cullis, T. D. Madden, M. Manoharan and M. J. Hope, *Angew. Chem., Int. Ed.*, 2012, **51**, 8529–8533.

50 N. Shobaki, Y. Sato and H. Harashima, *Int. J. Nanomed.*, 2018, **13**, 8395–8410.

51 M. A. Younis, Y. Sato, Y. H. A. Elewa and H. Harashima, *J. Controlled Release*, 2023, **361**, 592–603.

52 K. Hashiba, Y. Sato, M. Taguchi, S. Sakamoto, A. Otsu, Y. Maeda, T. Shishido, M. Murakawa, A. Okazaki and H. Harashima, *Small Sci.*, 2023, **3**, 2200071.

53 Y. Sato, N. Okabe, Y. Note, K. Hashiba, M. Maeki, M. Tokeshi and H. Harashima, *Acta Biomater.*, 2020, **102**, 341–350.

54 S. Chen, Y. Y. C. Tam, P. J. C. Lin, M. M. H. Sung, Y. K. Tam and P. R. Cullis, *J. Controlled Release*, 2016, **235**, 236–244.

55 J. Piella, N. G. Bastús and V. Puntes, *Bioconjugate Chem.*, 2017, **28**, 88–97.

56 S. Tenzer, D. Docter, J. Kuharev, A. Musyanovych, V. Fetz, R. Hecht, F. Schlenk, D. Fischer, K. Kiouptsi, C. Reinhardt, K. Landfester, H. Schild, M. Maskos, S. K. Knauer and R. H. Stauber, *Nat. Nanotechnol.*, 2013, **8**, 772–781.

57 V. P. Vu, G. B. Gifford, F. Chen, H. Benasutti, G. Wang, E. V. Groman, R. Scheinman, L. Saba, S. M. Moghimi and D. Simberg, *Nat. Nanotechnol.*, 2019, **14**, 260–268.

58 T. Ding, J. Guan, M. Wang, Q. Long, X. Liu, J. Qian, X. Wei, W. Lu and C. Zhan, *J. Controlled Release*, 2020, **319**, 371–381.

59 H. Matsui, Y. Sato, H. Hatakeyama, H. Akita and H. Harashima, *Int. J. Pharm.*, 2015, **495**, 171–178.

60 K. Okuda, Y. Sato, K. Iwakawa, K. Sasaki, N. Okabe, M. Maeki, M. Tokeshi and H. Harashima, *J. Controlled Release*, 2022, **348**, 648–659.

61 K. Sasaki, Y. Sato, K. Okuda, K. Iwakawa and H. Harashima, *Pharmaceutics*, 2022, **14**, 1572.

62 L. M. Kranz, M. Diken, H. Haas, S. Kreiter, C. Loquai, K. C. Reuter, M. Meng, D. Fritz, F. Vascotto, H. Hefesha, C. Grunwitz, M. Vormehr, Y. Hüsemann, A. Selmi, A. N. Kuhn, J. Buck, E. Derhovanessian, R. Rae, S. Attig, J. Diekmann, R. A. Jabulowsky, S. Heesch, J. Hassel, P. Langguth, S. Grabbe, C. Huber, Ö. Türeci and U. Sahin, *Nature*, 2016, **534**, 396–401.

63 U. Sahin, P. Oehm, E. Derhovanessian, R. A. Jabulowsky, M. Vormehr, M. Gold, D. Maurus, D. Schwarck-Kokarakis, A. N. Kuhn, T. Omokoko, L. M. Kranz, M. Diken, S. Kreiter, H. Haas, S. Attig, R. Rae, K. Cuk, A. Kemmer-Brück, A. Breitkreuz, C. Tolliver, J. Caspar, J. Quinkhardt, L. Hebich, M. Stein, A. Hohberger, I. Vogler, I. Liebig, S. Renken, J. Sikorski, M. Leierer, V. Müller, H. Mitzel-Rink, M. Miederer, C. Huber, S. Grabbe, J. Utikal, A. Pinter, R. Kaufmann, J. C. Hassel, C. Loquai and Ö. Türeci, *Nature*, 2020, **585**, 107–112.

64 K. J. Hassett, J. Higgins, A. Woods, B. Levy, Y. Xia, C. J. Hsiao, E. Acosta, Ö. Almarsson, M. J. Moore and L. A. Brito, *J. Controlled Release*, 2021, **335**, 237–246.

65 M. Mahmoudi, M. P. Landry, A. Moore and R. Coreas, *Nat. Rev. Mater.*, 2023, **8**, 422–438.

66 T. Kopac, *Int. J. Biol. Macromol.*, 2021, **169**, 290–301.

67 G. Bashiri, M. S. Padilla, K. L. Swingle, S. J. Shepherd, M. J. Mitchell and K. Wang, *Lab Chip*, 2023, **23**, 1432–1466.

68 C. Y. Zhang, W. G. Yuan, P. He, J. H. Lei and C. X. Wang, *World J. Gastroenterol.*, 2016, **22**, 10512–10522.

69 T. Tsuchida and S. L. Friedman, *Nat. Rev. Gastroenterol. Hepatol.*, 2017, **14**, 397–411.

70 S. Singh, N. Sharma, S. Shukla, T. Behl, S. Gupta, M. K. Anwer, C. Vargas-De-La-Cruz, S. G. Bungau and C. Brisc, *Molecules*, 2023, **28**, 2811.

71 S. Yazdani, R. Bansal and J. Prakash, *Adv. Drug Delivery Rev.*, 2017, **121**, 101–116.

72 M. A. Younis and H. Harashima, *Pharmacogenomics Pers. Med.*, 2024, **17**, 193–213.

73 Y. Sato, H. Hatakeyama, M. Hyodo and H. Harashima, *Mol. Ther.*, 2016, **24**, 788–795.

74 D. J. Gary, J. Min, Y. Kim, K. Park and Y.-Y. Won, *Macromol. Biosci.*, 2013, **13**, 1059–1071.

75 M. A. Younis, I. A. Khalil, Y. H. A. Elewa, Y. Kon and H. Harashima, *J. Controlled Release*, 2021, **331**, 335–349.

76 M. M. Abd Elwakil, I. A. Khalil, Y. H. A. Elewa, K. Kusumoto, Y. Sato, N. Shobaki, Y. Kon and H. Harashima, *Adv. Funct. Mater.*, 2019, **29**, 1970121.

77 A.-B. Marcher, S. M. Bendixen, M. K. Terkelsen, S. S. Hohmann, M. H. Hansen, B. D. Larsen, S. Mandrup, H. Dimke, S. Detlefsen and K. Ravnskjaer, *Sci. Rep.*, 2019, **9**, 2324.

78 Q. Cheng, T. Wei, L. Farbiak, L. T. Johnson, S. A. Dilliard and D. J. Siegwart, *Nat. Nanotechnol.*, 2020, **15**, 313–320.

79 S. Luozhong, Z. Yuan, T. Sarmiento, Y. Chen, W. Gu, C. McCurdy, W. Gao, R. Li, S. Wilkens and S. Jiang, *Nano Lett.*, 2022, **22**, 8304–8311.

80 O. S. Fenton, K. J. Kauffman, J. C. Kaczmarek, R. L. McClellan, S. Jhunjhunwala, M. W. Tibbitt, M. D. Zeng, E. A. Appel, J. R. Dorkin, F. F. Mir, J. H. Yang, M. A. Oberli, M. W. Heartlein, F. DeRosa, R. Langer and D. G. Anderson, *Adv. Mater.*, 2017, **29**, 1606944.

81 Y. Suzuki, M. Yakuwa, M. Sato, E. Samaridou, M. Beck-Broichsitter, M. Maeki, M. Tokeshi, Y. Yamada, H. Harashima and Y. Sato, *Next Nanotechnol.*, 2025, **8**, 100154.

82 Y. Suzuki, M. Yakuwa, M. Sato, E. Samaridou, M. Beck-Broichsitter, M. Maeki, M. Tokeshi, Y. Yamada, H. Harashima and Y. Sato, *J. Controlled Release*, 2025, **382**, 113687.

83 M. A. Younis, Y. Sato, Y. H. A. Elewa and H. Harashima, *Drug Delivery Transl. Res.*, 2025, DOI: **10.1007/s13346-025-01824-w.**

84 V. Fehring, U. Schaeper, K. Ahrens, A. Santel, O. Keil, M. Eisermann, K. Giese and J. Kaufmann, *Mol. Ther.*, 2014, **22**, 811–820.

85 S. A. Dilliard, Y. Sun, M. O. Brown, Y.-C. Sung, S. Chatterjee, L. Farbiak, A. Vaidya, X. Lian, X. Wang, A. Lemoff and D. J. Siegwart, *J. Controlled Release*, 2023, **361**, 361–372.

86 W. Tai, K. Yang, Y. Liu, R. Li, S. Feng, B. Chai, X. Zhuang, S. Qi, H. Shi, Z. Liu, J. Lei, E. Ma, W. Wang, C. Tian, T. Le, J. Wang, Y. Chen, M. Tian, Y. Xiang, G. Yu and G. Cheng, *Nat. Commun.*, 2023, **14**, 8042.

87 S. Omo-Lamai, M. E. Zamora, M. N. Patel, J. Wu, J. Nong, Z. Wang, A. Peshkova, A. Majumder, J. R. Melamed, L. S. Chase, E. O. Essien, D. Weissman, V. R. Muzykantov, O. A. Marcos-Contreras, J. W. Myerson and J. S. Brenner, *Adv. Mater.*, 2024, e2312026, DOI: **10.1002/adma.202312026.**

88 L. Xue, A. G. Hamilton, G. Zhao, Z. Xiao, R. El-Mayta, X. Han, N. Gong, X. Xiong, J. Xu, C. G. Figueroa-Espada, S. J. Shepherd, A. J. Mukalel, M. G. Alameh, J. Cui, K. Wang, A. E. Vaughan, D. Weissman and M. J. Mitchell, *Nat. Commun.*, 2024, **15**, 1884.

89 S. Kimura and H. Harashima, *Pharmaceutics*, 2020, **12**, 1216.

90 V. L. Feigin, T. Vos, E. Nichols, M. O. Owolabi, W. M. Carroll, M. Dichgans, G. Deuschl, P. Parmar, M. Brainin and C. Murray, *Lancet Neurol.*, 2020, **19**, 255–265.

91 S. M. Hoy, *Drugs*, 2019, **79**, 1255–1262.

92 C. A. Chiriboga, *Expert Rev. Neurother.*, 2017, **17**, 955–962.

93 J. Sevigny, P. Chiao, T. Bussière, P. H. Weinreb, L. Williams, M. Maier, R. Dunstan, S. Salloway, T. Chen, Y. Ling, J. O'Gorman, F. Qian, M. Arastu, M. Li, S. Chollate, M. S. Brennan, O. Quintero-Monzon, R. H. Scannevin, H. M. Arnold, T. Engber, K. Rhodes, J. Ferrero, Y. Hang, A. Mikulskis, J. Grimm, C. Hock, R. M. Nitsch and A. Sandrock, *Nature*, 2016, **537**, 50–56.

94 T. Okuyama, Y. Eto, N. Sakai, K. Nakamura, T. Yamamoto, M. Yamaoka, T. Ikeda, S. So, K. Tanizawa, H. Sonoda and Y. Sato, *Mol. Ther.*, 2021, **29**, 671–679.

95 W. M. Pardridge, *Trends Mol. Med.*, 2023, **29**, 343–353.

96 W. M. Pardridge, *Pharmaceutics*, 2022, **14**, 1283.

97 A. Salvati, A. S. Pitek, M. P. Monopoli, K. Prapainop, F. B. Bombelli, D. R. Hristov, P. M. Kelly, C. Aberg, E. Mahon and K. A. Dawson, *Nat. Nanotechnol.*, 2013, **8**, 137–143.

98 P. S. R. Naidu, N. Gavriel, C. G. G. Gray, C. A. Bartlett, L. M. Toomey, J. A. Kretzmann, D. Patalwala, T. McGonigle, E. Denham, C. Hee, D. Ho, N. L. Taylor, M. Norret, N. M. Smith, S. A. Dunlop, K. S. Iyer and M. Fitzgerald, *ACS Appl. Mater. Interfaces*, 2019, **11**, 22085–22095.

99 R. Dal Magro, B. Albertini, S. Beretta, R. Rigolio, E. Donzelli, A. Chiorazzi, M. Ricci, P. Blasi and G. Sancini, *Nanomedicine*, 2018, **14**, 429–438.

100 Z. Zhang, J. Guan, Z. Jiang, Y. Yang, J. Liu, W. Hua, Y. Mao, C. Li, W. Lu, J. Qian and C. Zhan, *Nat. Commun.*, 2019, **10**, 3561.

101 Z. A. Zhang, X. Xin, C. Liu, Y. H. Liu, H. X. Duan, L. L. Qi, Y. Y. Zhang, H. M. Zhao, L. Q. Chen, M. J. Jin, Z. G. Gao and W. Huang, *J. Nanobiotechnol.*, 2021, **19**, 453.

102 F. Ma, L. Yang, Z. Sun, J. Chen, X. Rui, Z. Glass and Q. Xu, *Sci. Adv.*, 2020, **6**, eabb4429.

103 X. Bian, L. Yang, D. Jiang, A. J. Grippin, Y. Ma, S. Wu, L. Wu, X. Wang, Z. Tang, K. Tang, W. Pan, S. Dong, B. Y. S. Kim, W. Jiang, Z. Yang and C. Li, *Nat. Commun.*, 2024, **15**, 3987.

104 X. Bian, Q. Guo, L. F. Yau, L. Yang, X. Wang, S. Zhao, S. Wu, X. Qin, Z. H. Jiang and C. Li, *Nat. Commun.*, 2025, **16**, 2368.

105 C. Wang, Y. Xue, T. Markovic, H. Li, S. Wang, Y. Zhong, S. Du, Y. Zhang, X. Hou, Y. Yu, Z. Liu, M. Tian, D. D. Kang, L. Wang, K. Guo, D. Cao, J. Yan, B. Deng, D. W. McComb, R. E. Parsons, A. M. Minier-Toribio, L. M. Holt, J. Pan, A. Hashemi, B. H. Kopell, A. W. Charney, E. J. Nestler, P. C. Peng and Y. Dong, *Nat. Mater.*, 2025, DOI: **10.1038/s41563-024-02114-5.**

106 Y. Kuzminich, A. Shakked, R. Calkins, S. Rudden, C. Jones, J. Doan, B. Jang, E. S. Echeverri, R. Zenhausern, L. Lian, D. Loughrey, H. E. Peck, R. Wiese, D. Koveal,

P. J. Santangelo and J. E. Dahlman, *Nano Res.*, 2024, **17**, 9126–9134.

107 P. Khare, S. X. Edgecomb, C. M. Hamadani, E. E. L. Tanner and D. S. Manickam, *Adv. Drug Delivery Rev.*, 2023, **197**, 114861.

108 S. Kimura and H. Harashima, *Neural Regener. Res.*, 2022, **17**, 785–787.

109 F. Piguet, T. de Saint Denis, E. Audouard, K. Beccaria, A. André, G. Wurtz, R. Schatz, S. Alves, C. Sevin, M. Zerah and N. Cartier, *Hum. Gene Ther.*, 2021, **32**, 349–374.

110 G. H. Petersen, S. K. Alzghari, W. Chee, S. S. Sankari and N. M. La-Beck, *J. Controlled Release*, 2016, **232**, 255–264.

111 X. Wang and W. Zhang, *J. Controlled Release*, 2022, **345**, 832–850.

112 X. Wang and W. Zhang, *J. Controlled Release*, 2022, **345**, 832–850.

113 M. A. Younis, I. A. Khalil, M. M. Abd Elwakil and H. Harashima, *Mol. Pharm.*, 2019, **16**, 4031–4044.

114 K. Zhou, L. H. Nguyen, J. B. Miller, Y. Yan, P. Kos, H. Xiong, L. Li, J. Hao, J. T. Minnig, H. Zhu and D. J. Siegwart, *Proc. Natl. Acad. Sci. U. S. A.*, 2016, **113**, 520–525.

115 H.-Y. Huang, L.-Q. Chen, W. Sun, H.-H. Du, S. Dong, A. M. Q. Ahmed, D. Cao, J.-H. Cui, Y. Zhang and Q.-R. Cao, *Theranostics*, 2021, **11**, 906–924.

116 Z. Pan, X. He, N. Song, D. Fang, Z. Li, J. Li, F. Luo, J. Li, H. Tan and Q. Fu, *ACS Appl. Mater. Interfaces*, 2019, **11**, 16421–16429.

117 W. Gao, C. M. Hu, R. H. Fang, B. T. Luk, J. Su and L. Zhang, *Adv. Mater.*, 2013, **25**, 3549–3553.

118 J. Zhuang, H. Gong, J. Zhou, Q. Zhang, W. Gao, R. H. Fang and L. Zhang, *Sci. Adv.*, 2020, **6**, eaaz6108.

119 H. T. Cheng, Y. N. Ngoc Ta, T. Hsia and Y. Chen, *Wiley Interdiscip. Rev.: Nanomed. Nanobiotechnol.*, 2024, **16**, e1953.

120 B. Du, X. Jiang, A. Das, Q. Zhou, M. Yu, R. Jin and J. Zheng, *Nat. Nanotechnol.*, 2017, **12**, 1096–1102.

121 R. Bruni, P. Possenti, C. Bordignon, M. Li, S. Ordanini, P. Messa, M. P. Rastaldi and F. Cellesi, *J. Controlled Release*, 2017, **255**, 94–107.

122 C. H. Choi, J. E. Zuckerman, P. Webster and M. E. Davis, *Proc. Natl. Acad. Sci. U. S. A.*, 2011, **108**, 6656–6661.

123 L. Guo, S. Luo, Z. Du, M. Zhou, P. Li, Y. Fu, X. Sun, Y. Huang and Z. Zhang, *Nat. Commun.*, 2017, **8**, 878.

124 V. Naumenko, A. Nikitin, K. Kapitanova, P. Melnikov, S. Vodopyanov, A. Garanina, M. Valikhov, A. Ilyasov, D. Vishnevskiy, A. Markov, S. Golyshev, D. Zhukov, I. Alieva, M. Abakumov, V. Chekhonin and A. Majouga, *J. Controlled Release*, 2019, **307**, 368–378.

125 A. Vasylaki, P. Ghosh, E. A. Jaimes and R. M. Williams, *Kidney360*, 2024, **5**, 618–630.

126 A. R. Chade and G. L. Bidwell 3rd, *Hypertension*, 2022, **79**, 1937–1948.

127 X. Han, L. Bi, J. Yan, P. Song, Y. Wang, X. Wang, Y. Wu, X. Ding, H. Zhang, Y. Wang and X. Li, *Mater. Today Bio*, 2024, **25**, 101002.

128 Y. Huang, J. Wang, K. Jiang and E. J. Chung, *J. Controlled Release*, 2021, **334**, 127–137.

129 A. Ruggiero, C. H. Villa, E. Bander, D. A. Rey, M. Bergkvist, C. A. Batt, K. Manova-Todorova, W. M. Deen, D. A. Scheinberg and M. R. McDevitt, *Proc. Natl. Acad. Sci. U. S. A.*, 2010, **107**, 12369–12374.

130 L. C. Chappell, C. A. Cluver, J. Kingdom and S. Tong, *Lancet*, 2021, **398**, 341–354.

131 K. L. Swingle, H. C. Safford, H. C. Geisler, A. G. Hamilton, A. S. Thatte, M. M. Billingsley, R. A. Joseph, K. Mrksich, M. S. Padilla, A. A. Ghalsasi, M.-G. Alameh, D. Weissman and M. J. Mitchell, *J. Am. Chem. Soc.*, 2023, **145**, 4691–4706.

132 N. Chaudhary, A. N. Newby, M. L. Arral, S. S. Yerneni, S. T. LoPresti, R. Doerfler, D. M. S. Petersen, C. Montoya, J. S. Kim, B. Fox, T. Coon, A. Malaney, Y. Sadovsky and K. A. Whitehead, *Proc. Natl. Acad. Sci. U. S. A.*, 2024, **121**, e2307810121.

133 K. L. Swingle, A. G. Hamilton, H. C. Safford, H. C. Geisler, A. S. Thatte, R. Palanki, A. M. Murray, E. L. Han, A. J. Mukalel, X. Han, R. A. Joseph, A. A. Ghalsasi, M. G. Alameh, D. Weissman and M. J. Mitchell, *Nature*, 2025, **637**, 412–421.

134 T. J. O'Toole and S. Sharma, in *StatPearls*, StatPearls Publishing, 2025, Copyright © 2025, StatPearls Publishing LLC., Treasure Island (FL) ineligible companies. Disclosure: Sandeep Sharma declares no relevant financial relationships with ineligible companies.

135 C. Leroux and G. Konstantinidou, *Cancers*, 2021, **13**, 799.

136 N. Sharma and V. Arora, *Pancreatology*, 2022, **22**, 937–950.

137 J. R. Melamed, S. S. Yerneni, M. L. Arral, S. T. LoPresti, N. Chaudhary, A. Sehrawat, H. Muramatsu, M. G. Alameh, N. Pardi, D. Weissman, G. K. Gittes and K. A. Whitehead, *Sci. Adv.*, 2023, **9**, eade1444.

138 Q. Shen, J. Liu, L. Zeng, Y. Ren, J. Liao, S. Chen, Y. Tang, Z. Zhang, M. Jiang, H. Liao, L. Wang, X. Xu and J. Chen, *J. Controlled Release*, 2025, **381**, 113588.

139 S. J. Morrison and D. T. Scadden, *Nature*, 2014, **505**, 327–334.

140 C. D. Sago, M. P. Lokugamage, F. Z. Islam, B. R. Krupczak, M. Sato and J. E. Dahlman, *J. Am. Chem. Soc.*, 2018, **140**, 17095–17105.

141 E. P. Cisneros, B. A. Morse, A. Savk, K. Malik, N. A. Peppas and O. L. Lanier, *J. Nanobiotechnol.*, 2024, **22**, 714.

142 M. Falahati, F. Attar, M. Sharifi, T. Haertlé, J. F. Berret, R. H. Khan and A. A. Saboury, *Biochim. Biophys. Acta, Gen. Subj.*, 2019, **1863**, 971–991.

143 S. A. Dilliard, Q. Cheng and D. J. Siegwart, *Proc. Natl. Acad. Sci. U. S. A.*, 2021, **118**, e2109256118.

144 K. Hashiba, M. Taguchi, S. Sakamoto, A. Otsu, Y. Maeda, Y. Suzuki, H. Ebe, A. Okazaki, H. Harashima and Y. Sato, *Nano Lett.*, 2024, **24**, 12758–12767.

145 K. Sasaki, Y. Sato, K. Okuda, K. Iwakawa and H. Harashima, *Pharmaceutics*, 2022, **14**, 1572.

146 S. Luozhong, Z. Yuan, T. Sarmiento, Y. Chen, W. Gu, C. McCurdy, W. Gao, R. Li, S. Wilkens and S. Jiang, *Nano Lett.*, 2022, **22**, 8304–8311.

147 M. Qiu, Y. Tang, J. Chen, R. Muriph, Z. Ye, C. Huang, J. Evans, E. P. Henske and Q. Xu, *Proc. Natl. Acad. Sci. U. S. A.*, 2022, **119**, e2116271119.

148 L. Xue, A. G. Hamilton, G. Zhao, Z. Xiao, R. El-Mayta, X. Han, N. Gong, X. Xiong, J. Xu, C. G. Figueroa-Espada, S. J. Shepherd, A. J. Mukalel, M.-G. Alameh, J. Cui, K. Wang, A. E. Vaughan, D. Weissman and M. J. Mitchell, *Nat. Commun.*, 2024, **15**, 1884.

149 A. A. H. Abdellatif, A. Bouazzaoui, H. M. Tawfeek and M. A. Younis, *Colloids Surf., B*, 2024, **238**, 113930.

150 R. M. Williams, J. Shah, B. D. Ng, D. R. Minton, L. J. Gudas, C. Y. Park and D. A. Heller, *Nano Lett.*, 2015, **15**, 2358–2364.